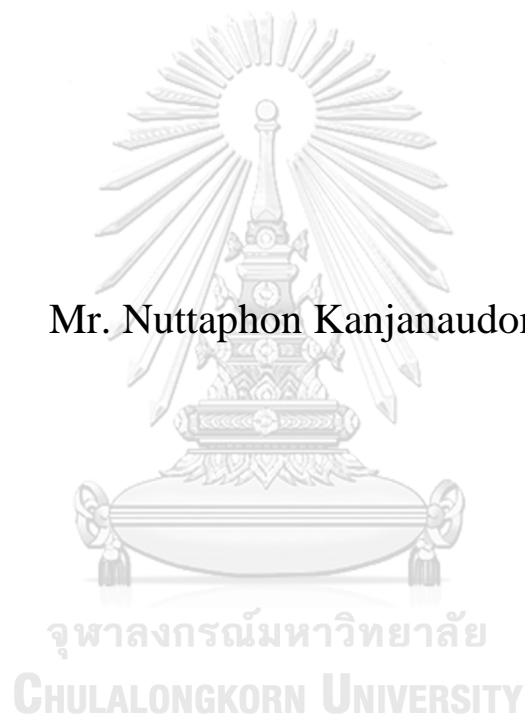


COMPUTATIONAL FLUID DYNAMICS MODELING OF THE CLIMATE INSIDE A CHICKEN HOUSE

Mr. Nuttaphon Kanjanaudomsuk



A Thesis Submitted in Partial Fulfillment of the Requirements  
for the Degree of Master of Engineering in Chemical Engineering  
Department of Chemical Engineering  
Faculty of Engineering  
Chulalongkorn University  
Academic Year 2018  
Copyright of Chulalongkorn University

การจำลองพลศาสตร์ของไหลของสภาพอากาศภายในโรงเรียนเลี้ยงไก่



วิทยานิพนธ์นี้เป็นส่วนหนึ่งของการศึกษาตามหลักสูตรปริญญาวิศวกรรมศาสตรมหาบัณฑิต  
สาขาวิชาวิศวกรรมเคมี ภาควิชาวิศวกรรมเคมี  
คณะวิศวกรรมศาสตร์ จุฬาลงกรณ์มหาวิทยาลัย  
ปีการศึกษา 2561  
ลิขสิทธิ์ของจุฬาลงกรณ์มหาวิทยาลัย

Thesis Title                                    COMPUTATIONAL FLUID DYNAMICS MODELIN  
    G OF THE CLIMATE INSIDE A CHICKEN HOUSE  
By    Mr. {Nuttaphon Kanjanaudomsuk  
Field of Study                                    Chemical Engineering  
Thesis Advisor                                   Pimporn Ponpesh, Ph.D.

---

Accepted by the Faculty of Engineering, Chulalongkorn University in Partial  
Fulfillment of the Requirement for the Master of Engineering

..... Dean of the Faculty of Engineering  
(Associate Professor SUPOT  
TEACHAVORASINSKUN, D.Eng.)

THESIS COMMITTEE

..... Chairman  
(Assistant Professor Apinan Soottitantawat, Ph.D.)  
..... Thesis Advisor  
(Pimporn Ponpesh, Ph.D.)  
..... Examiner  
(Assistant Professor Sompong Putivisutisak, Ph.D.)  
..... Examiner  
(Pongtorn Charoensuppanimit, Ph.D.)  
..... External Examiner  
(Chanikarn Wongviriyawong, Ph.D.)



จุฬาลงกรณ์มหาวิทยาลัย  
CHULALONGKORN UNIVERSITY

ณัฐพล กาญจนอุดมสุข : การจำลองพลศาสตร์ของไหลของสภาพอากาศภายในโรงเรือนเลี้ยงไก่.

(  
COMPUTATIONAL FLUID DYNAMICS MODELING OF T  
HE CLIMATE INSIDE A CHICKEN HOUSE) อ.ที่ปรึกษาหลัก : อ.

ดร.พิมพ์พร พลเพชร

ผลิตภัณฑ์จากไก่ในปัจจุบันส่วนมากมาจากการเลี้ยงในโรงเรือนแบบปิด สภาพอากาศในโรงเรือนแบบนี้จะส่งผลต่อสุขภาพของไก่ คุณภาพและปริมาณของผลิตภัณฑ์จากไก่อย่างมาก โดยเฉพาะอย่างยิ่งในประเทศไทยซึ่งตั้งอยู่ในภูมิอากาศเขตร้อนชื้น ฟาร์มไก่แบบปิดมักประสบปัญหาจากสภาวะเครียดเนื่องจากความร้อน (Thermal stress) ในไก่ ดังนั้นการดำเนินงานภายในโรงเรือนและการออกแบบโรงเรือนเพื่อให้สามารถควบคุมสภาพอากาศภายในโรงเรือนให้เหมาะสมต่อการเติบโตของไก่จึงมีความสำคัญอย่างยิ่งยวด ซึ่งการศึกษาสภาพอากาศภายในโรงเรือนสามารถทำได้โดยการจำลองพลศาสตร์ของไหลเชิงคำนวณ ในงานวิจัยนี้ได้ศึกษาปัจจัยที่ส่งผลต่อสภาพอากาศภายในโรงเรือน ซึ่งประกอบด้วยความเร็ว อุณหภูมิ และความชื้นสัมพัทธ์ของอากาศ โดยอาศัยสมการการเคลื่อนที่แบบปั่นป่วน (Realizable k- $\epsilon$  turbulent model) สมการอนุรักษ์พลังงาน และสมการการถ่ายโอนมวลสาร ทั้งนี้ได้มีการยืนยันความถูกต้องของแบบจำลองด้วยการเปรียบเทียบผลการทำนายกับผลการเก็บข้อมูลจริงภายในโรงเรือนเลี้ยงไก่ จากผลการเปรียบเทียบโดยการคำนวณค่า Normalize mean square error (NMSE) พบว่าผลการทำนายมีความสอดคล้องกันกับข้อมูลจริง ยกเว้นความเร็วของอากาศได้แก่พื้นที่ลมซึ่งอาจเนื่องมาจากข้อจำกัดของเครื่องมือวัดความเร็วอากาศและความสามารถของแบบจำลองในการคำนวณความปั่นป่วนที่เกิดจากการไหลแบบเจ็ท จากนั้นจึงใช้แบบจำลองที่ผ่านการยืนยันความถูกต้องในการออกแบบแนวทางการดำเนินงานและรูปแบบโรงเรือนเพื่อให้สามารถรักษาสภาพอากาศภายในโรงเรือนให้เหมาะสมสำหรับการเจริญเติบโตของไก่ โดยเฉพาะในสภาพอากาศภายนอกที่รุนแรง โดยดัชนีที่ใช้บ่งชี้ความเหมาะสมของสภาพอากาศคือค่า Effective temperature จากผลการออกแบบแนวทางการดำเนินงานทำให้สามารถระบุการทำงานของ Evaporative cooling pad และจำนวนพัดลมที่เหมาะสมสำหรับสภาพอากาศภายในโรงเรือนที่เปลี่ยนแปลงไปในรอบปีได้ นอกจากนี้ การปรับปรุงโรงเรือนด้วยการติดตั้งฉนวนกันความร้อนช่วยให้สามารถป้องกันการถ่ายความร้อนจากหลังคาเข้าสู่โรงเรือน และการปรับปรุงแผ่นซึ่งลมสามารถช่วยเพิ่มความเร็วของอากาศที่พัดผ่านตัวไก่ การปรับปรุงโรงเรือนด้วยการติดตั้งฉนวนกันความร้อนร่วมกับการปรับปรุงแผ่นซึ่งลมช่วยให้สามารถลดค่า Effective temperature ให้อยู่ในช่วงที่เหมาะสมแม้ในสภาพอากาศภายนอกที่รุนแรงได้ นอกจากนี้ การปรับปรุงโรงเรือนยังช่วยเพิ่มความสม่ำเสมอของสภาพอากาศในบริเวณที่มีไก่ ซึ่งช่วยให้เกิดการกระจายตัวที่เหมาะสมของไก่ด้วย

สาขาวิชา วิศวกรรมเคมี

ลายมือชื่อนิติ

ปีการศึกษา 2561

ลายมือชื่อ อ.ที่ปรึกษาหลัก

# # 5970388221 : MAJOR CHEMICAL ENGINEERING

KEYWORD CFD, Chicken house, Ventilation system

D:

Nuttaphon Kanjanaudomsuk :  
 COMPUTATIONAL FLUID DYNAMICS MODELING OF THE CLIMATE INSIDE A CHICKEN HOUSE. Advisor: Pimporn Ponpesh, Ph.D.

Nowadays, most of chicken products are from a closed house system. Climate inside such chicken house can significantly affect chicken welfare and its productivity. Moreover, Thailand is in a tropical region where thermal stress is easily occurred. Suitable operating condition and chicken house design can help improve interior climate which can be evaluated by computational fluid dynamics (CFD) modeling technique. In this study, realizable  $k-\epsilon$  model, energy conservation and species transport equations were applied to simulate the air velocity, temperature and relative humidity, respectively, inside the chicken house. The model was validated with measured air velocity, temperature and relative humidity inside the chicken house during real farming operation. Good agreements, based on the values of normalized mean square error (NMSE), between simulation results and measured data were found, except the air velocity beneath the deflectors. The deviation might be due to the limitation of the air velocity sensor and the capability to predict eddies due to jet flow of the turbulence model. The validated model was then applied to develop an operational guideline and design improvement to maintain the favorable indoor climate for chicken even in extreme environment. The effective temperature was considered as an indicator for suitable climates for the chicken. The results showed that the developed operational guideline for evaporative cooling pad and exhaust fans could help maintain favorable indoor climate in all weather conditions throughout the years. In addition, an installation of thermal insulation could help mitigate the heat transfer from the roof. A design modification to the wind deflectors could also increase the air velocity and improve the ventilation. With both thermal insulation and deflector modification, the effective temperature at the chicken level could be maintained within the optimal range even in severe weather condition. Furthermore, it also improved the uniformity of the indoor climate in the chicken occupied zone, and thus enhanced well-distribution of the chicken.

Field of Study:	Chemical Engineering	Student's Signature
		.....
Academic Year:	2018	Advisor's Signature
		.....

## ACKNOWLEDGEMENTS

This thesis could not be successful without the kindness of these people. First, I would like to thank my advisor, Dr. Pimporn Ponpesh, who made inspiration in simulation work, guidance, encouragement and continuing support of this thesis from the start until success. Besides my advisor, I would like to thank the rest of my committees, Asst. Prof. Dr. Sompong Putivisutisak, Asst. Prof. Dr. Apinan Soottitantawat, Dr. Pongtorn Charoensuppanimit and Dr. Chanikarn Wongviriyawong for their insightful comments, invaluable guidance in technical problems, and hard questions. In addition, the author is also grateful for Better Foods Company Limited and teams for giving me the great opportunity to work on diversely exciting projects and for providing support, assistance, facilities and materials for the experiments. I would like to thank Mr. Sutkhet Eksuk, Mr. Sawas, Mr. Mongkol, Mr. Surasuk Thakerd and Mr. Pornthep Chongkol for their insightful comments, and their helps in providing facilities and materials for the experiments.

Finally, my graduation would not be achieved without best wishes from my parents, who help me with everything and always give me greatest love and financial support until the completion of this study.

# TABLE OF CONTENTS

	<b>Page</b>
ABSTRACT (THAI) .....	iii
ABSTRACT (ENGLISH).....	iv
ACKNOWLEDGEMENTS.....	v
TABLE OF CONTENTS.....	vi
CHAPTER 1 INTRODUCTION .....	1
1.1 Motivation.....	1
1.2 Objectives of the research.....	3
1.3 Scopes of the research .....	3
1.4 Benefits of this research.....	3
CHAPTER 2 THEORY AND LITERATURE REVIEW .....	4
2.1 Closed house chicken farming.....	4
2.1.1 Environmental impact on chicken.....	4
2.1.2 Operation in closed house chicken farming .....	7
2.2 Chicken house simulation using CFD modeling .....	8
2.3 Computational fluid dynamics.....	9
2.3.1 Pre-processor.....	10
2.3.2 Solver.....	11
2.3.3 Post-processor .....	13
2.4 Governing equations.....	13
2.5 Turbulence modeling in animal house.....	14
2.6 Animal occupied zone in CFD model .....	17
2.7 Heat and humidity emitted from the chickens and the litter.....	18
2.8 Discrete phase model.....	19
2.9 CFD validation.....	21
CHAPTER 3 MATERIAL AND METHODS.....	22

3.1 Computational method.....	22
3.1.1 System description .....	22
3.1.2 Modeling of chicken house .....	23
3.1.3 Animal occupied zone modeling.....	28
3.1.4 Operating condition design and chicken house improvement.....	28
3.1.5 Two-stage cooling system .....	29
3.2 Experimental method .....	30
CHAPTER 4 RESULTS AND DISCUSSIONS.....	31
4.1 Grid independent study.....	31
4.2 Animal occupied zone modeling .....	32
4.3 CFD validation.....	33
4.3.1 Air velocity validation.....	33
4.3.2 Air temperature and relative humidity validation .....	36
4.4 CFD simulation.....	40
4.4.3 Effective temperature at the chicken level .....	44
4.5 Operating condition guideline .....	45
4.6 Chicken house simulation in extreme climate condition.....	47
4.7 Modification of the chicken house .....	50
4.7.1 Thermal insulation.....	50
4.7.2 Deflector modification .....	53
4.7.3 Tunnel door modification.....	59
4.7.4 Two-stage cooling system .....	67
CHAPTER 5 CONCLUSIONS AND RECOMMENDATION .....	69
5.1. Conclusions.....	69
5.2 Recommendations.....	70
REFERENCES .....	71
REFERENCES .....	77
Appendix A.....	78



Appendix B .....	79
Appendix C .....	81
VITA .....	84



# CHAPTER 1

## INTRODUCTION

### 1.1 Motivation

In 2017, Thailand is the 6<sup>th</sup> frozen chicken exporter in the world [1]. In addition, the processed chicken and frozen chicken was the 5<sup>th</sup> and 7<sup>th</sup> Thai exported agriculture product, respectively [2]. The growth rate of chicken product exporting has increased continuously since 2004 after the outbreak of avian influenza (Office of Agricultural Economics, OAE, 2017).

Nowadays, most of chicken products are from a closed house system. It provides more benefits such as a good interior climate control, a good feed control, high level biosecurity, and high quality and quantity products [3, 4]. However, the key factor which indicate a chicken production level is its welfare [5]. An interior environment has an effect on the chicken welfare. Temperature and relative humidity are the main factors. There is a report that temperature and relative humidity affects a chicken health, growth rate and production rate [6-8]. Moreover, Thailand is in a tropical region where thermal stress and pathogenic pollution are easily occurred. Therefore, an interior climate control and improvement are crucial topics to make the chicken welfare and production better and to decrease its mortality.

An efficient ventilation system can help improve the climate inside the chicken house. A sufficient air velocity can induce humidity and heat transfer from inside to outside of the chicken house due to the convective transport. The one topic which is needed to be concerned is a uniformity of the climate. A non-uniform of climate makes chicken flock, leading to overcrowding and increasing the mortality of the chicken. Moreover the overcrowding makes the chicken compete to get food and water. This causes the deviation in chicken growth. The deviation results in poor quality products.

The investigation of the climate inside the chicken house can be conducted by using Computational Fluid Dynamics (CFD) modelling technique. CFD is a numerical

method to calculate problems involving transport phenomena. Recently, CFD has been used to study the climate and ventilation system in livestock building [3, 9-13]. The one reason which makes CFD a powerful technique is that it provides a result in 3-dimensions for analysis and increases an efficiency of system design and modification.

There are several earlier works on chicken houses using CFD modeling. However, many studies on the tunnel ventilation system chicken houses with are only consider air velocity and temperature [14-19]. Most industrial farms in the tropical region use ventilation system and humidity significantly influences the interior air quality. Thus, it is important to investigate this ventilation system including humidity distribution in the house to promote the chicken productivity and reduce the mortality for farms in the tropical region. In addition, the uniform of climate condition in the house is favorable condition for chicken production. It is necessary to study and develop the modified interior design of the house for climate improvement. According to Rojano et al., the flow resistance from the chicken is more significant due to the high density of the chicken inside the house [10]. Moreover, the tunnel ventilation system provides high air velocity [15]. This flow resistance due to the chicken is much more significant. But there are a few studies which concerned this resistance in the CFD chicken house model [20]. A practical equipment for increase air velocity inside the tunnel ventilation system house is deflector. The deflector was installed to reduce the airflow cross sectional area which makes the air flow with higher velocity. But the studies on the influence of the deflector on the air flow are limited [17, 21, 22].

In this research, a tunnel ventilation close chicken house is studied using CFD technique. Heat and humidity generated by chicken and litter are considered in the model. In addition, a porous media is used to represent a chicken occupied zone and its flow resistance. The effect of the deflector on airflow is concerned. The model is validated by comparing the simulation results with the experimental data including velocity, temperature and relative humidity profiles in the chicken house. Normalized mean square error (NMSE) is considered as an indicator of prediction accuracy. The validated model is applied to develop a design and operational guideline to maintain favorable climate inside the chicken house.

## **1.2 Objectives of the research**

- 1.2.1 To develop a CFD model which can well predict the transport phenomena in a chicken house.
- 1.2.2 To suggest a design improvement and operational guideline to maintain favorable climate, which is suitable for the chicken inside the chicken house.

## **1.3 Scopes of the research**

- 1.3.1 Develop a CFD model to solve the transport phenomena, i.e., momentum, heat, and mass transfers in the chicken house.
- 1.3.2 Validate the model by comparing air velocity, temperature and humidity estimated from CFD simulations with the measured values from the experiments to check the accuracy of the model.
- 1.3.3 Apply the validated model to investigate profiles of air velocity, temperature and relative humidity in the house.
- 1.3.4 Apply the validated model to design interior equipment of the chicken house (for example deflector dimension and arrangement, number of fan, etc.) and operating condition in order to improve the climate condition and to achieve favorable effective temperature.

## **1.4 Benefits of this research**

- 1.4.1 To be able to predict the airflow profile, distribution of temperature and humidity in the chicken house.
- 1.4.2 To obtain guidelines to help improve the climate condition in the chicken house and mitigate the thermal stress problem.

## CHAPTER 2

### THEORY AND LITERATURE REVIEW

#### 2.1 Closed house chicken farming

##### 2.1.1 Environmental impact on chicken

In chicken industry, a chicken welfare is very important topic to be concerned. The good chicken welfare results in good chicken health and production [23]. There are many factors which affect chicken welfare. One of the factors which plays an important role is an interior climate in a chicken house [5]. The temperature above 30 °C cause heat stress for chicken especially in a hot region [8]. Heat stress is a main problem which result in high mortality of the chickens. In addition, Mashaly et al. reported that the reduction of body weight and feed consumption are significant affected by heat stress. The heat stress not only decrease chicken production but also inhibits immune function which cause chicken mortality [7]. D.F. Pereira and I.A. Naas studied the thermo neutral zone for broiler breeders by analysis the chicken behavior (e.g. drinking water and movement). The study showed that the chicken drink more and move less when the temperature is above the thermo neutral zone represented as **Figure 2.1.1**.

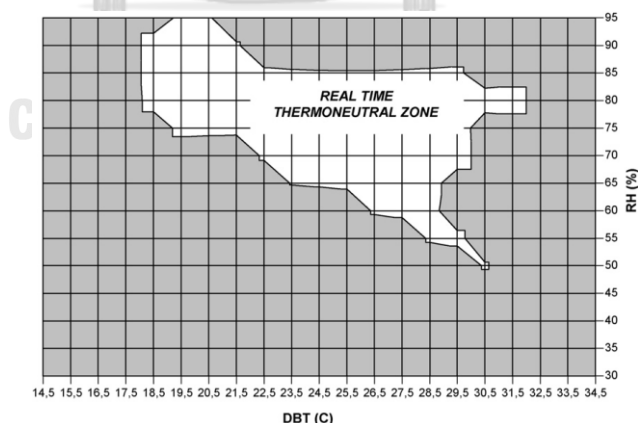


**Figure 2.1.1** Broiler breeder thermo neutral zone studied by D.F. Pereira and I.A. Naas [24]

An air velocity in the house is also a key role which affect the chicken welfare. Increasing the air velocity is a practical technique to improving chicken welfare when temperatures are high enough to cause heat stress. An increase in air velocity can more

induce a convective heat loss reducing temperature around the chicken [25]. May et al. reported that the chicken exposed to the high air velocity has more weight and consume less water and more feed [23]. Yahav S. et al. also founded that the chickens exposed to high air velocity gain more weight [26]. However, the heat stress cannot be solved by increasing air velocity when the air temperatures are above 37.7°C and the highest effective temperature which can be reduce heat stress is 35°C [27].

An effect of relative humidity on the chicken results in their natural behavior. At high temperature and high relative humidity cause a reduction in evaporation rate of chicken leading to increasing chicken heat stress. High relative humidity increases litter moisture and ammonia concentrations. Moreover, a risk of infection of chicken is increased with relative humidity because it is a favorable condition of infectivity of pathogens [6].

To indicate the level of chicken welfare, Tao and Xiuping developed Temperature-Humidity-Velocity index or THVI to integrates the effect of air temperature, humidity and velocity on the homeostasis of the birds [28]. In the past, Temperature-humidity index was developed to indicate the level of climate which affect to various animals such as cows [29], pigs [30] and laying hens [31]. But the air velocity have a massive role in heat convection especially the house with ventilation system [28]. Therefore, the air velocity should be integrated in the index for cover all factors which affect on the chicken. THVI equation can be represented as Eq. (1)

$$THVI = (0.85 \times t_{db} + 0.15 \times t_{wb}) \times V^{-0.058} \quad (0.2 \leq V \leq 1.2) \quad (1)$$

Where  $t_{db}$  is dry-bulb temperature,  $t_{wb}$  is wet-bulb temperature and  $V$  is air velocity.

$t_{db}$  can be represented by  $T$  in energy conservation equation (Eq. (6)).  $t_{wb}$  can be calculated from  $T$  and relative humidity (RH%) which is expressed in Eq. (2) [32].

$$t_{wb} = T \tan^{-1} \left[ 0.151977 \left( RH\% + 8.313659 \right)^{\frac{1}{2}} \right] + \tan^{-1}(T + RH\%) \\ - \tan^{-1}(RH\% - 1.676331) + 0.00391838 (RH\%)^{\frac{3}{2}} \tan^{-1}(0.023101 RH\%) \\ - 4.686035 \quad (2)$$

The THVI can indicate the level of chicken welfare by calculating the core body temperature changes ( $t_b$ ). The response of the core body temperature of the chicken to environmental climate can be calculated from THVI as Eq. (3).  $\Delta t_{b(90)}$  represents the core body temperature change during the first 90 minute exposure.

$$\Delta t_{b(90)} = 0.39 \times THVI - 12.22 \quad (3)$$

The core body temperature changes ( $\Delta t_b$ ) of 1.0, 2.5, 4.0 and  $>4.0^\circ\text{C}$  are classified for normal, alert, danger and emergency state of homeostasis, respectively. The exposure time (ET, min) for the core body change of each state can be calculated by Eq. (4-6).

$$\text{For } \Delta t_b = 1.0^\circ\text{C}, \quad ET = 2 \times 10^{29} \times THVI^{-17.68} \quad (4)$$

$$\text{For } \Delta t_b = 2.5^\circ\text{C}, \quad ET = 4 \times 10^{13} \times THVI^{-7.38} \quad (5)$$

$$\text{For } \Delta t_b = 4.0^\circ\text{C}, \quad ET = 3 \times 10^{11} \times THVI^{-5.91} \quad (6)$$

Although the THVI can represent many aspect of the environmental effect on the chicken, the range of the air temperature in Tao and Xiuping experiments is not cover the range of the air temperature in this study.

Beside the THVI, the effective temperature represents the level of the climate impact which couples the effect of air velocity, temperature, relative humidity on the chicken. The idea of the effective temperature is that at the same real temperature the animal feels the temperature differently if the air velocity or relative humidity around them is different. As mention above, the airflow can induce the heat convection from the chicken which make the chicken feel the temperature below than the real temperature. The effective temperature can be calculated from the correlation of air velocity and temperature as presented in Eq. (7-9) which is classified by the relative humidity level. These equation are achieved by using the regression of raw data (see **Appendix A**) [33]. The suitable effective temperature range is  $21 \pm 3$  degree Celsius.

For relative humidity  $< 50$  percent

$$ET = 1.30T - 0.247v - 0.007T^2 + 0.851v^2 - 0.198vT - 2.498 \quad (7)$$

For relative humidity 50 - 70 percent

$$ET = 2.11T + 1.43v - 0.019T^2 + 0.7v^2 - 0.246vT - 14.67 \quad (8)$$

For relative humidity > 70 percent

$$ET = 1.76T + 2.01v - 0.011T^2 + 0.471v^2 - 0.247vT - 10.07 \quad (9)$$

Where ET is effective temperature.

### 2.1.2 Operation in closed house chicken farming

The air velocity and temperature are keys for closed house chicken farming especially for the farm in hot and tropical region. An air velocity can be manipulated by the number of operated fans responded to the air temperature. At the high temperature, the number of fans must be high in order to provide higher air velocity for carrying the heat from the inside to the outside of the house. And at the lower temperature, the increasing air velocity may be risky because the chicken become chilled which make them sit down and stop eating [23].

However, only the air velocity may be not effective to prevent the thermal stress when the external air temperature is extremely high. The widely used method for reducing incoming air temperature is evaporative cooling pad system. The high temperature air is drawn into a pad. During the process, the water is sprayed continuously on the porous pad. The water consumes heat from the air in order to evaporate from the pad. Thus, the hot air is changed to the cool moist air. The evaporative cooling pad efficiency is defined as the ratio of the actual air temperature decrease and the maximum of the air temperature decrease. The lowest of the air temperature which can be decreased is the wet-bulb temperature of input air. Thus, the efficiency of evaporative cooling system can be expressed as Eq. (10) [34].

$$\epsilon = \frac{T_{in} - T_{out}}{T_{in} - T_{wb}} \quad (10)$$

Where  $\epsilon$  is evaporative cooling system efficiency;  $T_{in}$  is the input air temperature;  $T_{out}$  is the air temperature from the pad;  $T_{wb}$  is the wet-bulb temperature of input air.



In this study, the evaporative cooling pad efficiency was assumed to be 85 percent. The assumption was proved by statistical analysis expressed in **Appendix B**.

## **2.2 Chicken house simulation using CFD modeling**

Livestock building studies by CFD has become popular in recent years (e.g. cattle building [13, 35], pig barn [36-38] and chicken [9, 11, 18, 39]). It is important to study climate condition and ventilation in livestock building but it is very complicated to directly investigate due to limitation of equipment. CFD modeling technique has a powerful ability for investigation the transport phenomena and fluid flow. Therefore, the climate condition and air ventilation inside livestock building study can be studied by CFD modeling effectively. The CFD modeling can provide the 3-D results which is useful to study and visualize the system. Moreover, the validated model can be used as a prototype for simulation the system modification or the system with the different condition.

There are various type of the chicken house which depends on the ventilation system. The external climate and desired air velocity inside the house are key factors to determine the type of ventilation system. The cross-ventilation system chicken house was studied by many researchers [3, 11, 19, 39]. V. Blanes-Vidal et al. simulated the air velocity distribution inside the cross-ventilated chicken house. The simulation results showed a good agreement with the experimental data [19]. However, the simulation and experiment were conduct in the house without the chicken precise and temperature and humidity distribution were not considered in the model. Fernando Rojano simulated a two-dimensional cross ventilation chicken house [3]. This model was considered effect of outside climate at any time. The heat, humidity and CO<sub>2</sub> emitted from chicken, litter and heater were considered in this model. But the chicken was not modeled. The prediction from simulated model were in good agreement with experimental data. The single-sided ventilation in chicken house was investigated by Eliseo Bustamante et al. [40]. The air velocity distribution was simulated and the validated model was applied to simulate the effect of the fan diffusers on the velocity distribution.

In this study, the researcher focuses on the tunnel ventilation system chicken house. The tunnel ventilation system is suitable for the farm in the tropical region where the climate is hot and humid, because it can provide high air velocity distributed along the house. Eliseo Bustamante et al. studied the air flow inside the empty house [15]. The simulated air velocity was compared with experimental data. The ANOVA showed that there was no difference between simulation and experiment. According to the author, CFD techniques provided the information for improvement the climate in the house. However, the simulation and experiment were conducted in the house without the chicken precise and temperature and humidity distribution were not considered in the model. The airflow velocity and temperature distribution inside the tunnel-ventilated chicken house were studied by Jairo Alexander Osorio Saraz et al. [14], Robinson Osorio Hernandez et al. [18], Huifeng Zou et al. [22] and Milan Zajicek and Pavel Kic [17]. But all of these studies were not concerned the effect of the flow resistance by the chicken. The flow resistance becomes significant if an amount animal in the house is high enough [10]. In tunnel ventilation system chicken house, the practical technique for an air velocity improvement is installation of deflectors. Huifeng Zou et al. [22] and Milan Zajicek and Pavel Kic [17] simulated the air velocity and temperature inside the tunnel-ventilated chicken house with deflectors. The results showed that the deflector installation can help increase the air velocity so that the air flow can induce more heat convection from the chicken to the outside of the house. However, the simulation was not validated with experimental results.

From the above literature reviews, this research aims to study the air velocity, temperature and relative humidity distribution inside the tunnel-ventilation system chicken house. The heat and humidity emitted from the chicken and litter are considered in this study. The flow resistance by the chicken is modeled as an animal occupied zone. Moreover, the effect of the deflectors on airflow is investigated and validated with the experimental data.

### **2.3 Computational fluid dynamics**

Computational fluid dynamics or CFD is a technique which solves problems involving fluid flow and transport phenomena. This technique is well-known as a

powerful tool in the field of research and equipment design and spans a wide range of application areas. There are many benefits of CFD in fluid system design:

- Reducing time and costs of new design developments or experiments
- Ability to model complicated systems or systems that is difficult or impossible to do experiments
- Ability to provide results in three dimensions

The CFD processes contain of three main steps: pre-processor, solver and post-processor [41].

### 2.3.1 Pre-processor

Pre-processing is to define the flow problems to a CFD program. The required information for definition of the problems consists of the computational domain, grid generation, physical and chemical phenomena that are needed to be modelled, fluid and material properties and boundary condition.

For example, the computation domain is a rod as shown in **Figure 2.3.1**. Then the domain is divided into discrete control volumes as shown in **Figure 2.3.2**.



**Figure 2.3.1** Computational domain

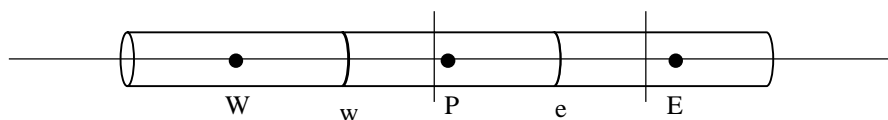


**Figure 2.3.2** Generated grid

A cell center or general node is identified by point P. Point W and E are neighbor node. The side faces of the control volume are represented by w and e.

### 2.3.2 Solver

In this step, the numerical method is applied to compute the transport phenomena in the fluid flow. Generally, the governing equations are partial differential equations (PDEs). PDEs cannot be solved directly. It is needed a numerical method to convert PDEs into algebraic equation which can be solve. The solver computes the set of algebraic equations iteratively until the systems are reached an acceptable convergence.

A numerical method selected in this study is Finite volume method (FVM) which is the most commercial CFD code. The concept of FVM is consist three step as the following:

- Integration of the governing equations over all the control volumes of the domain.
- Discretization which is conversion of partial differential equations into algebraic equations.
- Applying an iterative method to solve the algebraic equation

The solver applies several algorithms to compute the set of algebraic equations. The solver algorithms are describe by the following:

#### 1) Overview of flow solvers

The users have to choose one of the two numerical methods: pressure-based solver and density-based solver. The approach of these methods used to solve the discretized equations is different.

The pressure-based approach was for low-Mach number incompressible flows, while the density-based approach was mainly used for high-Mach number compressible flows. The velocity field is obtained from the momentum equations in both methods.

In the density-based approach, the continuity equation is used to obtain the density field. The pressure field is determined from the equation of state. On the other hand, in the pressure-based approach, the pressure field is solved by pressure or pressure correction equation which is obtained by coupling continuity and momentum equations.

## 2) Discretization

Generally, the discrete values of the scalar variable are stored at the cell center. But the face values required for the convection terms must be interpolated from the cell center values. There are several upwind scheme to achieve this values. The “upwind” means that the face value is derived from the cell upstream value. The users have to choose the upwind scheme which consists of first-order upwind, second-order upwind, power law and QUICK. To choose the discretization scheme depend on desired accuracy and calculation time. The summary of each scheme is described in the following.

- First-order upwind scheme: the cell faces value is assumed to be the upstream cell-center value.
- Power-law scheme: The face values is determined using the exact solution to a one-dimensional convection-diffusion equation.
- Second-order upwind scheme: The cell faces value are computed using a multidimensional linear construction approach. In this approach, higher-order accuracy is achieved at cell faces through a Taylor series expansion of the cell-centered solution about the cell centroid.
- Central-Differencing scheme: The cell faces value is calculated from the average of the nearby cell center value and the average of the nearby cell center value gradient.
- QUICK scheme: QUICK schemes are based on a weighted average of second-order upwind and central interpolations of the variable.

## 3) Pressure-velocity coupling

In general computation, the pressure field is a part of the solution, so its gradient is not normally known. The pressure field calculation is related to continuity equation and momentum equation. The coupling between pressure and velocity is a constraint in the solution of the flow field. If the correct pressure field is applied in the momentum equations the resulting velocity field should satisfy continuity. There are several pressure-velocity coupling algorithms: SIMPLE, SIMPLEC, PISO and Coupled. The chosen algorithm depend on the behavior of the problem and calculation time.

### 2.3.3 Post-processor

The post-processor provides 2-D or 3-D data as visualization result, geometry and grid display, vector plot, line and shaded contour plots, etc. at each and every point in the domain.

## 2.4 Governing equations

The mathematical statements of the conservation laws of physics represent the governing equations of fluid flow. Mass conservation equation (continuity equation) can be expressed by Eq. (11).

$$\frac{\partial \rho}{\partial t} + \nabla \cdot (\rho u) = 0 \quad (11)$$

The general conservation equation of variable  $\phi$  in the system can be expressed by Eq. (12).

$$\frac{\partial(\rho\phi)}{\partial t} + \nabla \cdot (\rho\phi u) = \nabla \cdot (\Gamma \nabla \cdot \phi) + S_\phi \quad (12)$$

Where  $u$  is velocity and  $\Gamma$  is diffusion coefficient. The first and second term on left side of the equation represent time-dependent component and convection component respectively. The first and second term on right side of the equation represent diffusion component and source component respectively. The variable  $\phi$  depend on the variable of interest in fluid flow (e.g. momentum, energy and species transport).

Momentum conservation equation (Equation of motion) can be expressed by Eq. (13).

$$\rho \frac{Du}{Dt} = -\nabla p + \nabla \cdot \tau + S_M \quad (13)$$

Where  $p$  and  $\tau$  are pressure and viscous stress of fluid respectively.  $S_M$  is momentum source term.

For Newtonian and incompressible fluid, equation of motion can be rearrange into Navier-Stokes equation. The equation expressed by Eq. (14).

$$\rho \frac{\partial u}{\partial t} + \rho(u \cdot \nabla u) = -\nabla p + \mu \nabla^2 u + S_M \quad (14)$$

Where  $\mu$  is fluid viscosity.

Energy conservation equation can be expressed by Eq. (15)

$$\rho \hat{C}_p \frac{DT}{Dt} = -(\nabla \cdot q) - (\tau : \nabla u) - \left( \frac{\partial \ln \rho}{\partial \ln T} \right)_p \frac{Dp}{Dt} + S_h \quad (15)$$

Where  $\hat{C}_p$  is the specific heat capacity;  $q$  is heat flux;  $S_h$  is a source term which includes the heat of chemical reaction and any other volumetric heat sources and  $T$  is temperature.

For incompressible fluid inviscid fluid, the Eq. (5) can be expressed by Eq. (16)

$$\rho \hat{C}_p \frac{DT}{Dt} = -(\nabla \cdot q) + S_h \quad (16)$$

Species transport equation of  $i^{\text{th}}$  species can be expressed by Eq. (7)

$$\frac{\partial(\rho Y_i)}{\partial t} + \nabla \cdot (\rho u Y_i) = -\nabla \cdot J_i + R_i + S_i \quad (17)$$

Where  $Y_i$  represent mass fraction of species  $i$  and  $R_i$  is the net rate of production of species  $i$ .  $S_i$  is source term of mass of species  $i$ .

## 2.5 Turbulence modeling in animal house

The flow regime in the animal house is turbulent especially the ventilated house. Generally, the Navier-stokes equation cannot solve the turbulence of the flow [42]. Reynolds average method is one of approach which calculate the turbulent quantities and rely on additional equation. The k- $\epsilon$  turbulent model is one of the most widely model for prediction of turbulent in animal livestock building [3, 4, 9, 12, 15, 39, 40, 43]. The k- $\epsilon$  model family contains of standard k-  $\epsilon$ , RNG k-  $\epsilon$  and realizable k-  $\epsilon$  model. However, Li H. et al. studied the accuracy of model applied various turbulent model in animal house simulation by comparing the simulated result with experimental data [37]. The result showed that the RNG deviated from other models and experiment in prediction of the airflow pattern. The realizable k- $\epsilon$  is chosen in this study because it is developed from standard k- $\epsilon$  model to improve the prediction for rotating and recirculation flow [44].

For Reynolds (ensemble) averaging approach, the solution variables in the instantaneous Navier-Stokes equation are decomposed into the mean and fluctuating components. Eq. (18) shows the velocity component.

$$u_i = \bar{u}_i + \acute{u}_i \quad (18)$$

Where  $\bar{u}_i$  and  $\acute{u}_i$  are the mean and fluctuating velocity component respectively.

For pressure and other scalar quantities ( $\phi$ ) can be written as Eq. (19).

$$\phi = \bar{\phi} + \acute{\phi} \quad (19)$$

Substitute this velocity variable form into the instantaneous continuity and momentum equation and take an ensemble average over the equations. Then, the equations become Eq. (20) and Eq. (21) called Reynolds-averaged Navier-Stokes (RANS) equation.

$$\frac{\partial \rho}{\partial t} + \frac{\partial}{\partial x_i} (\rho \bar{u}_i) = 0 \quad (20)$$

$$\begin{aligned} & \frac{\partial}{\partial t} (\rho \bar{u}_i) + \frac{\partial}{\partial x_j} (\rho \bar{u}_i \bar{u}_j) \\ &= -\frac{\partial p}{\partial x_i} + \frac{\partial}{\partial x_j} \left[ \mu \left( \frac{\partial \bar{u}_i}{\partial x_j} + \frac{\partial \bar{u}_j}{\partial x_i} - \frac{2}{3} \delta_{ij} \frac{\partial \bar{u}_l}{\partial x_l} \right) \right] + \frac{\partial}{\partial x_j} (-\rho \overline{\acute{u}_i \acute{u}_j}) \end{aligned} \quad (21)$$

These equation have the same general form as the instantaneous Navier-stokes equations. An additional term in Eq. (21) called Reynolds stress expresses the effects of the turbulence. It must be modeled in order to close this term.

A common method used to model Reynolds stresses is the Boussinesq hypothesis showed in Eq. (22).

$$-\rho \overline{\acute{u}_i \acute{u}_j} = \mu_t \left( \frac{\partial \bar{u}_i}{\partial x_j} + \frac{\partial \bar{u}_j}{\partial x_i} \right) - \frac{2}{3} \left( \rho k + \mu_t \frac{\partial \bar{u}_k}{\partial x_k} \right) \delta_{ij} \quad (22)$$

An assumption of the Boussinesq hypothesis is that the turbulent viscosity ( $\mu_t$ ) is an isotropic scalar quantity. The turbulent viscosity is solved by additional equation. In this study, the k- $\epsilon$  model which contain two additional equations (for the turbulence kinetic energy, k and the turbulence dissipation rate,  $\epsilon$ ) is used to calculate turbulent viscosity. In case of k- $\epsilon$  model, there are three types of this model: 1) standard k- $\epsilon$



model 2) RNG k- $\varepsilon$  model and 3) Realizable k- $\varepsilon$  model. The Realizable k- $\varepsilon$  is chosen because this model has substantial improvement over the standard k- $\varepsilon$  model. The improvement features include strong streamline curvature, vortices and rotation. The realizable k- $\varepsilon$  equation model contains an alternative formulation for the turbulent viscosity. A modified equation for the dissipation rate ( $\varepsilon$ ) based on an exact solution for the transport of the mean-square vorticity fluctuation.

The turbulence kinetic energy and turbulence dissipation rate are shown in Eq. (23) and Eq. (24) respectively.

$$\frac{\partial}{\partial t}(\rho k) + \frac{\partial}{\partial x_j}(\rho k u_j) = \frac{\partial}{\partial x_j} \left[ \left( \mu + \frac{\mu_t}{\sigma_k} \right) \frac{\partial k}{\partial x_j} \right] + G_k + G_b - \rho \varepsilon - Y_M + S_k \quad (23)$$

$$\begin{aligned} & \frac{\partial}{\partial t}(\rho \varepsilon) + \frac{\partial}{\partial x_j}(\rho \varepsilon u_j) \\ &= \frac{\partial}{\partial x_j} \left[ \left( \mu + \frac{\mu_t}{\sigma_\varepsilon} \right) \frac{\partial \varepsilon}{\partial x_j} \right] + \rho C_1 S_\varepsilon - \rho C_2 \frac{\varepsilon^2}{k + \sqrt{\nu \varepsilon}} + C_{1\varepsilon} \frac{\varepsilon}{k} C_{3\varepsilon} G_b + S_\varepsilon \end{aligned} \quad (24)$$

$$\text{Where } C_1 = \max \left[ 0.43, \frac{\eta}{\eta + 5} \right], \eta = S \frac{k}{\varepsilon}, S = \sqrt{2S_{ij}S_{ij}}$$

$G_k$  represents the generation of turbulence kinetic energy due to the mean velocity gradients.  $G_b$  is the generation of turbulence kinetic energy due to buoyancy.  $Y_M$  represents the contribution of the fluctuating dilation in compressible turbulence to the overall dissipation rate.  $C_2$  and  $C_{1\varepsilon}$  are constants.  $\sigma_k$  and  $\sigma_\varepsilon$  are the turbulent Prandtl numbers for  $k$  and  $\varepsilon$ , respectively.  $S_k$  and  $S_\varepsilon$  are user-defined source terms.

The model constants have been developed to make the model performs well. The model constant are  $C_{1\varepsilon} = 1.44$ ,  $C_2 = 1.9$ ,  $\sigma_k = 1.0$ ,  $\sigma_\varepsilon = 1.2$

The turbulent viscosity is computed from Eq. (25). The difference between the realizable k- $\varepsilon$  and the standard and RNG k- $\varepsilon$  models is that  $C_\mu$  is not constant. It is a function of the mean strain and rotation rates, the angular velocity of the system rotation, and the turbulence variable ( $k$  and  $\varepsilon$ ).

$$\mu_t = \rho C_\mu \frac{k^2}{\varepsilon} \quad (25)$$

## 2.6 Animal occupied zone in CFD model

For chicken house modelling, the chicken behavior must be considered. The animal occupied zone (AOZ) can be modelled in various method. Some studies model the chicken house to investigate air velocity, temperature and relative humidity without considering animal or only heat and humidity produced by chicken [3, 4, 11, 12, 15, 19, 39, 40]. Although it is simply method to not consider animal occupied zone, there is an effect of chicken on the airflow direction [45]. Modeling the animal as an actual or simplified geometry is a method that make the animal closed to the reality. There are some research that approach this method to model the animals such as cows [46], pigs [36] and chicken in the cage or modules [9]. Nonetheless, this method is practical for small scale livestock facilities [45]. Modeling all of chickens in the chicken house as an actual size is too difficult and complicated. The alternate method is considered the AOZ as a porous media. Mendes L. et al. modeled the cow in a naturally ventilated barn as a porous media [47]. The model showed the realistic air flow patterns within the barn. The benefits of the porous media is that this method can represent the flow resistance from the animal. Rojano F. et al. suggested that the resistance in chicken house becomes significant if an amount animal in the house is high enough [10]. Thus, the porous media is a proper representation of the AOZ with high density of chicken. However, this approach requires additional coefficient which is viscous and inertial term for modeling the porous media. Cheng Q. et al. investigated the air flow resistance from chicken using CFD and claimed that the resistance coefficient obtained from this study can be applied to related simulation study [45].

The porosity of porous media is based on void between the chicken zone and the volume of the chicken. The chicken is assumed to be sphere of which surface area can be estimated by Eq. (26) [48]. Then the volume of the chicken is calculated from the surface area of the sphere.

$$A_s = 0.081m^{0.667} \quad (26)$$

Where  $A_s$  is surface area of sphere ( $m^2$ ) and  $m$  is mass of the chicken ( $kg$ ).

The additional source term for porous media in equation of motion is applied and can be expressed by Eq. (27). The first and second term of this equation are viscous loss term and inertial loss term, respectively.

$$S_m = \frac{\Delta P}{L} = - \left( C_v \mu u_i + C_i \frac{1}{2} \rho |u| u_i \right) \quad (27)$$

Where  $\frac{\Delta P}{L}$  is pressure drop per length;  $C_i$  is the viscous resistance coefficient;  $C_i$  is the inertial resistance coefficient;  $u$  is velocity of fluid;  $|u|$  is magnitude of velocity;  $\mu$  is viscosity of fluid and  $\rho$  is density of fluid.

## 2.7 Heat and humidity emitted from the chickens and the litter

In the chicken house, the fresh air from outside is impaired by the heat and humidity emitted from the chickens. Pedersen S. and Sällvik, K. suggested an estimation for total heat from chicken which can be expressed by Eq. (28) [49]. The total heat ( $\Phi_{tot, watt}$ ) is estimated from mass of chicken and environmental temperature around the chicken.

$$\Phi_{tot} = 10.62 m^{0.75} (1 + (20/1000)(20 - T)) \quad (28)$$

Where  $m$  is the chicken mass (kg) and  $T$  is temperature around the chicken ( $^{\circ}C$ ).

The total heat can be divided into sensible heat and latent heat. The sensible heat ( $\Phi_s$ ) can be calculated from the total heat and can be expressed in Eq. (29). The latent heat ( $\Phi_l$ ) is a residual between the total heat and the sensible heat which can be expressed in Eq. (30). The latent heat from the chickens indicates the amount of humidity emitted from the chicken.

$$\Phi_s = 0.62 \Phi_{tot} - (0.228/1000)T^2 \quad (29)$$

$$\Phi_l = \Phi_{tot} - \Phi_s \quad (30)$$

As same as the chicken, the heat and humidity are also emitted from the litter. The total heat from the litter is approximated about 10 percent of the total heat produced by the chicken (Eq. 28) and the amount of heat can be divided into 60 percent and 40

percent for sensible and latent heat, respectively [50]. The heat from the chicken and the litter is represented by the source term in the energy conservation equation.

## 2.8 Discrete phase model

Generally, the humidity produced by chicken is water droplet in exhale breath from respiration system. This liquid droplet has to be properly modeled to specify the heat transport between it and environment correctly. The droplet is in a liquid phase and vaporizes in to the air. The amount of vapor is represented in the species transport equation and the latent heat for vaporization is represented in the energy conservation equation source term.

The discrete phase model is applied to simulate the particle (or droplet or bubble) as a discrete second phase which is dispersed in the continuous phase (air). The equation of motion for particles is defined by the force balance on the particle which can be expressed in Eq. (31).

$$\frac{du_p}{dt} = F_D(u - u_p) + \frac{g(\rho_p - \rho)}{\rho_p} + F \quad (31)$$

Where  $u_p$  is the particle velocity,  $u$  is the fluid velocity,  $\rho_p$  is the density of particle and  $\rho$  is the fluid density.

$F$  is an additional acceleration term,  $F_D(u - u_p)$  is the drag force per unit particle mass.  $F_D$  can be calculated from Eq. (32) and  $\frac{g(\rho_p - \rho)}{\rho_p}$  is sum of buoyancy force and gravitational force.

$$F_D = \frac{18\mu}{\rho_p d_p^2} \frac{C_D Re}{24} \quad (32)$$

Where  $\mu$  is fluid viscosity,  $d_p$  is the particle diameter,  $C_D$  is drag coefficient and  $Re$  is relative Reynolds number which is defined as Eq. (33).

$$Re = \frac{\rho d_p |u_p - u|}{\mu} \quad (33)$$

The vaporization of liquid droplet is initiated when the temperature of the droplet reaches the vaporization temperature and continues until the droplet reaches the boiling point or is completely consumed. Because of high vaporization rate, the

vaporization mechanism applied in simulation software is convective/diffusion controlled model. The vaporization rate can be expressed in Eq. (34).

$$\frac{dm_p}{dt} = k_c A_p \rho_\infty \ln(1 + B_m) \quad (34)$$

Where  $m_p$  is droplet mass,  $A_p$  is droplet surface area,  $\rho_\infty$  is density of bulk gas and  $B_m$  is the Spalding mass number which expressed by Eq. (35).

$$B_m = \frac{Y_{i,s} - Y_{i,\infty}}{1 - Y_{i,s}} \quad (35)$$

Where  $Y_{i,s}$  is vapor mass fraction at the surface and  $Y_{i,\infty}$  is vapor mass fraction in the bulk gas.

The mass transfer coefficient ( $k_c$ ) is calculated from the Sherwood number correlation written by Eq. (36)

$$Sh_{Ab} = \frac{k_c d_p}{D_{i,m}} = 2.0 + 0.6 Re^{1/2} Sc^{1/3} \quad (36)$$

Where  $D_{i,m}$  is diffusion coefficient of vapor in the bulk and  $Re$  is relative Reynolds number (Eq. (33))  $Sc$  is the Schmidt number (Eq. (37)).

$$Sc = \frac{\mu}{\rho D_{i,m}} \quad (37)$$

A droplet heat balance relates the sensible heat change in the droplet to the convective and latent heat transfer between the droplet and the continuous phase. The energy equation for droplet is written as Eq. (38).

$$m_p c_p \frac{dT_p}{dt} = h A_p (T_\infty - T_p) - \frac{dm_p}{dt} h_{fg} \quad (38)$$

Where  $c_p$  is droplet heat capacity,  $T_p$  is droplet temperature,  $T_\infty$  is temperature of continuous phase,  $h$  is convective heat transfer coefficient,  $\frac{dm_p}{dt}$  is vaporization rate and  $h_{fg}$  is latent heat of vaporization.

The convective heat transfer coefficient ( $h$ ) can be calculated from a modified Nusselt number (Nu) correlation expressed in Eq. (39).

$$Nu = \frac{hd_p}{k_\infty} = \frac{\ln(1+B_T)}{B_T} (2 + 0.6Re_d^{1/2} Pr^{1/3}) \quad (39)$$

Where  $k_\infty$  is thermal conductivity of the continuous phase,  $B_T$  is the Spalding heat transfer number which is assumed to be equal to the Spalding mass transfer number ( $B_m$ ).  $Pr$  is Prandtl number of the continuous phase (Eq. (40)).

$$Pr = \frac{c_p \mu}{k_\infty} \quad (40)$$

## 2.9 CFD validation

The validation of simulation results can be conducted by several method. The aims of validation is to ensure that the simulation can predict the results well. In this study, the simulation results of air velocity, temperature and relative humidity at various location were compared with the experimental data. Consistency between CFD simulation and experiment were evaluated by calculation the normalized mean square error (NMSE). There were many CFD simulation study that applied the NMSE for validation as statistical analysis [12, 14, 16]. The NMSE can be computed by Eq. (41). The value of NMSE less than 0.25 are considered as good indicators of consistency.

$$NMSE = \frac{1}{N} \frac{\sum_n (C_{pi} - C_{oi})^2}{(C_{pm} \cdot C_{om})} \quad (41)$$

Where

$$C_{pm} = \frac{1}{N} \sum_i C_{pi} \quad (42)$$

$$C_{om} = \frac{1}{N} \sum_i C_{oi} \quad (43)$$

$N$  is number of data.  $C_{pi}$  and  $C_{oi}$  are predicted and measured values, respectively.

## CHAPTER 3

### MATERIAL AND METHODS

The CFD simulation processes consist of creating the computational domain of chicken house and generating grids before setting up the simulation using Fluent. The simulation results will be validated with the experimental data. The validated model will be used as a based model in order to modify the geometry of the chicken house and operating conditions.

#### 3.1 Computational method

##### 3.1.1 System description

The computational domain of the CFD model was based on an existing chicken house, which contained 8000 chickens and used evaporative cooling pad for decreasing inlet temperature. The dimension of the chicken house is indicated in **Figure 3.1.1**. The air flowed through the both sides of inlet to outlet due to exhaust fans. The deflectors were installed to deflect the wind direction. The installation of the deflector was started at the length of 21 meters from the front of the house, the next ones were at every 6 meters and the last one was at 105 meters. **Figure 3.1.2** shows the cross-sectional view of the chicken house. There is a wire mesh gate at 48 meters from the front of the chicken house. The floor is covered with a rice husk. The height of the rice husk is gradually increased due to the influence of the exhaust fans.

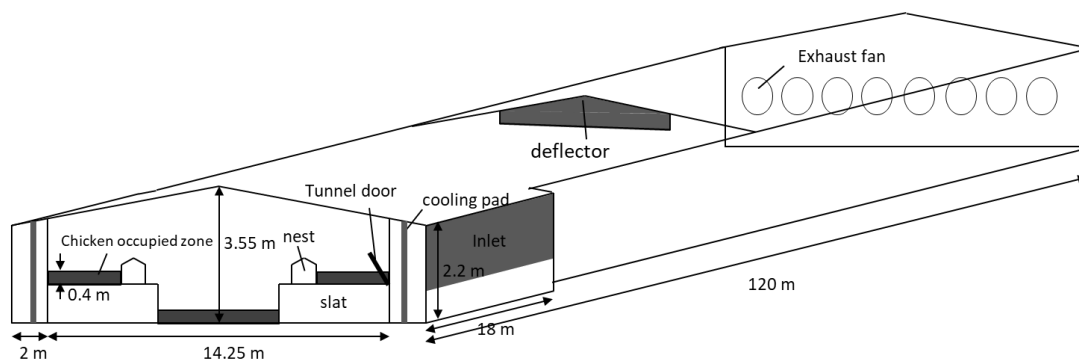


**Figure 3.1.1** Dimension of the chicken house

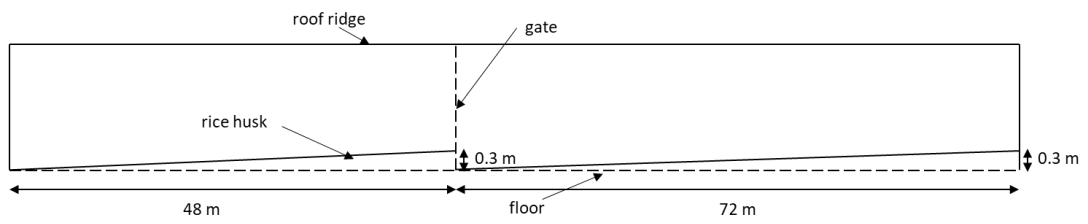


**Figure 3.1.2** Cross-sectional view of the chicken house

### 3.1.2 Modeling of chicken house

#### 3.1.2.1 Pre-processor

1) Use Ansys Workbench 18.1 (Workbench 18.1, ANSYS Inc., Lebanon, NH) to draw the computational domain as an actual size. The computational domain is shown in **Figure 3.1.2**.

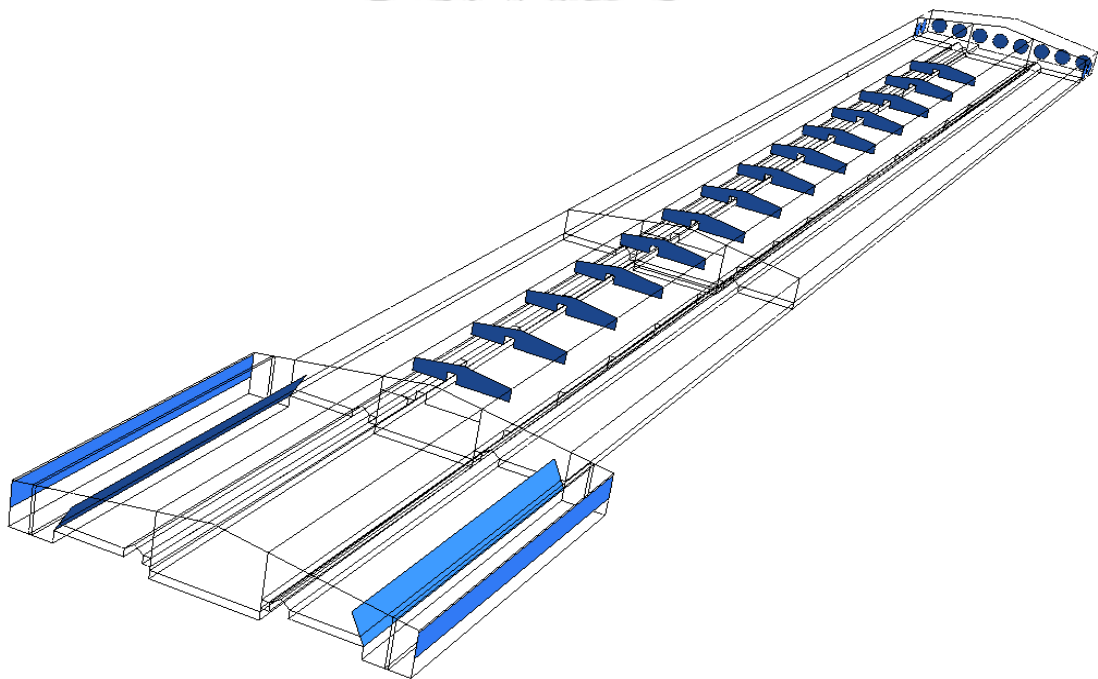


**Figure 3.1.2** Geometry drawn by Workbench 18.1



2) Generate computational meshes. The meshed geometry is shown in **Figure 3.1.3**.



**Figure 3.1.3** Meshed geometry

3) Grid independent study

The geometry is divided into small elements or grids. The grid resolution affects the accuracy of the prediction. The coarse grids can lead to inaccuracy or wrong prediction. It is necessary to study whether the grids are fine enough. This study is called “grid independent study”. The number of grids used in this study contain 3 level; coarse (1334000 elements), medium (2693000 elements) and fine (3700000 elements). Each grid was used to simulate the air velocity profile inside a chicken house.

4) Define boundary condition and material properties.

The boundary conditions are described in **Table 3.1.1** and Fluid properties are described in **Table 3.1.2**.

**Table 3.1.1** Boundary condition and cell zone condition

Type	Parameter	Value
Air inlet	Velocity (m/s)	1.5
	Temperature (degree Celsius)	26.5
	Relative humidity (percent)	73
Exhaust fan	Pressure jump	$-1.60 v^2 + 1.31 v + 124.03$ [51]
Wall	Temperature (degree Celsius)	29.4
Floor	Heat flux (W/m <sup>2</sup> )	0
Roof	Temperature (degree Celsius)	29.2
Chicken	Weight (kg)	Male : 4.42, Female : 3.64
	Surface area (m <sup>2</sup> )	Male : 0.192, Female : 0.218
	Number of chicken	Male : 700, Female : 7300
	Emitted heat (Watt/m <sup>3</sup> )	237.89
	Emitted humidity (kgH <sub>2</sub> O/s)	0.0383
Evaporative cooling pad	Type	Porous media
	Inertial resistance coefficient (m <sup>-1</sup> )	1.13e-04 [52]
	Viscous resistance coefficient (m <sup>-2</sup> )	3.3e+06 [52]

**Table 3.1.2** Fluid properties

Species	Properties	Value <sup>a</sup>
Oxygen	Molecular weight (kg/kmol)	31.99
Nitrogen	Molecular weight (kg/kmol)	28.01
Water (vapor)	Molecular weight (kg/kmol)	18.02
Air	Density (kg/m <sup>3</sup> )	1.176 <sup>b</sup>
	Specific heat capacity (j/kg K)	1006.43
	Thermal conductivity (W/m K)	0.024
	Viscosity (kg/m s)	1.79e-05
Water droplet (liquid)	Molecular weight	28.97
	Density (kg/m <sup>3</sup> )	998.2
	Specific heat capacity (j/kg K)	4182
	Thermal conductivity (W/m K)	0.6
	Viscosity (kg/m s)	0.001
	Latent heat (kJ/kg)	2263.07
	Vaporization temperature (K)	284
	Boiling point (K)	373
	Binary diffusivity (m <sup>2</sup> /s)	Film-averaged
	Saturation vapor pressure (pa)	Piecewise-linear

a: fluent database

b: reference temperature = 300.15 K

### 3.1.2.2 Solver

1) The governing equations and additional source term used in this model are described in **Chapter 2**.

2) The model assumptions are the following:

- Steady state flow
- Incompressible and Newtonian fluid
- No slip condition
- Uniform chicken distribution
- Spherical droplet and uniform size of droplet.

- Droplet interaction was neglected.
- Thermophoretic force and Brownian force were neglected in DPM.
- No chemical reaction occurred

3) Some of numerical schemes are showed in **Table 3.1.3**. The SIMPLE algorithm was chosen because it is general and suitable for steady state problem. Pressure field was calculated by using PRESTO scheme because it suitable for swirling flow. The second order upwind scheme was chosen because this scheme provides more accuracy than first order upwind and take not much computational time.

**Table 3.1.3** Numerical scheme

Discretization	Scheme
Pressure-velocity coupling	SIMPLE
Pressure	PRESTO
Momentum	Second order upwind
Turbulent kinetic energy	Second order upwind
Turbulent dissipation rate	Second order upwind
Species	Second order upwind
Energy	Second order upwind

### 3.1.2.3 Post-processor

- 1) The simulation results is compared with the experimental results to validate the model.
- 2) Contour of velocity, temperature and relative humidity and vector of airflow is used to investigate the climate profile in the chicken house [3, 16].
- 3) Contour of velocity, temperature and relative humidity in each section in horizontal and vertical plane is used to observe the uniformity of climate [3].

### 3.1.3 Animal occupied zone modeling

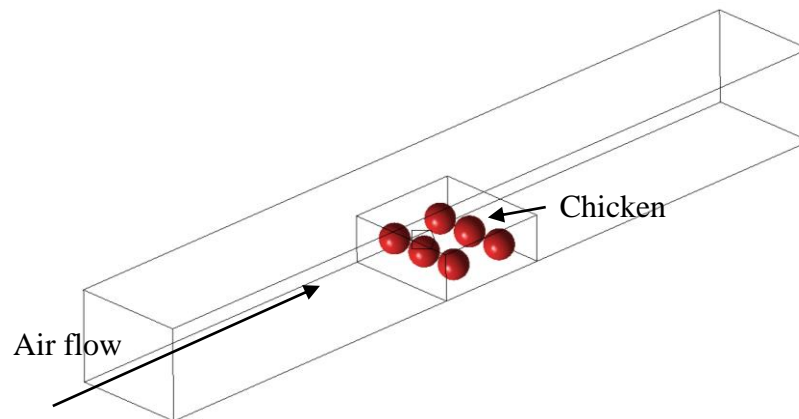


**Figure 3.1.4** Animal occupied zone modeling

In this study, the animal occupied zone is considered as a porous media. The pressure drop due to the resistance of the porous media can be expressed as Eq. (27). The permeability and inertial resistance factor can be calculated by applying sub-model. The sub-model is used to simulate the air flow through the chicken as shown in **Figure 3.1.4**. A chicken is modeled as a sphere. A radius was calculated by Eq. (26). The inlet velocity is varied by 1, 1.5, 2 and 2.5 m/s and the pressure drop by the chicken at each inlet velocity are calculated. The permeability and inertial resistance factor are achieved by regression between pressure drop and velocity.

### 3.1.4 Operating condition design and chicken house improvement

After the validation was conducted, the validated model was applied to investigate as following.

- Study the air velocity, temperature and relative humidity distribution and analyse the effect of the equipment on the airflow inside the house.
- Develop an operational guideline to maintain a favorable climate for the chicken when the external climate changes in a year period.
- Simulate the interior climate to study the factors which cause the unsuitable climate inside the house when the external climate is at extreme condition.
- Guide the modification of the chicken house in order to improve the climate inside the chicken house when the external climate is at extreme condition.

### 3.1.5 Two-stage cooling system

Other improvements to further reduce the effective temperature in severe weather condition might be done by additional cooling system to reduce the heat from the inlet air. A preliminary study has been conducted on a two stages cooling system as shown in **Figure 3.1.5**. It consists of an air to soil heat exchanger and an evaporative cooling pad. First, the air is drawn by an exhaust fan through a duct which is buried at a 2.5 - 3 meters deep underground. At the depth of 2.5 - 3 meters, the soil temperature is lower than the air temperature and constant throughout the year [53]. After sufficient amount of heat is transferred from the air, it is delivered to the evaporative cooling pad to further decrease the temperature. The advantage of the first cooling step, i.e., the air-to soil heat exchanger, is that it does not increase the humidity in the air so that the air temperature can be further decreased by the evaporative cooling pad.

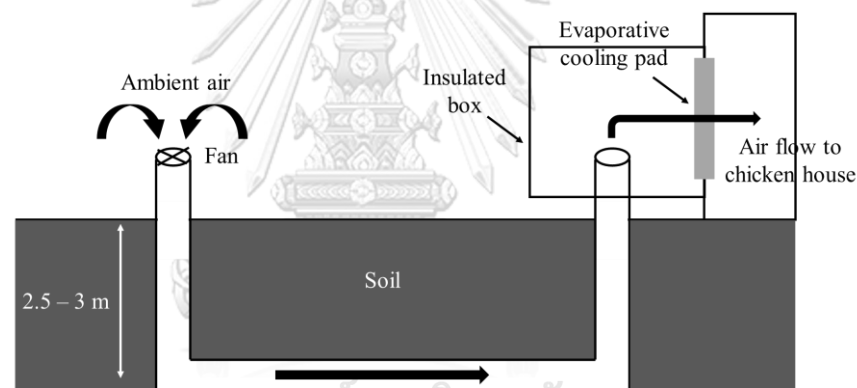


**Figure 3.1.5** Two-stage cooling system

In the preliminary study, the effect of the pipe length on the air temperature decrease by using CFD simulation. The soil is at a constant temperature of 22.4 degree Celsius [54]. The inlet air temperature and relative humidity (extreme external climate) was 41 degree Celsius and 40 percent, respectively [55, 56]. The pipe material was stainless steel with 0.762 meter outside diameter and 6.35 millimeters thick (ASME standard). The duct air inlet velocity was 6 m/s ( $2.7 \text{ m}^3/\text{s}$ ). The duct length was varied at 20, 25 and 30 meters.

### 3.2 Experimental method

For model validation, the experiment was conducted to measure the variables that indicate the climate condition. The variables consist of velocity, temperature and relative humidity. Instruments for measurement these variables are the following:

- 1) Velocity
  - Velocicalc 9565 Thermoanemometer probe
- 2) Temperature & Relative humidity
  - Velocicalc 9565 VOC, temperature, CO<sub>2</sub> and humidity probe

The measurement locations was divided into 4 sections of the chicken house. Each section consisted of nine points of which three points at the middle, three other points are on the left and the other three points are on the right. The measurement points are shown in **Figure 3.2.1**. The measurement height were at 0.3 (at chicken head level) and 1.4 meters.

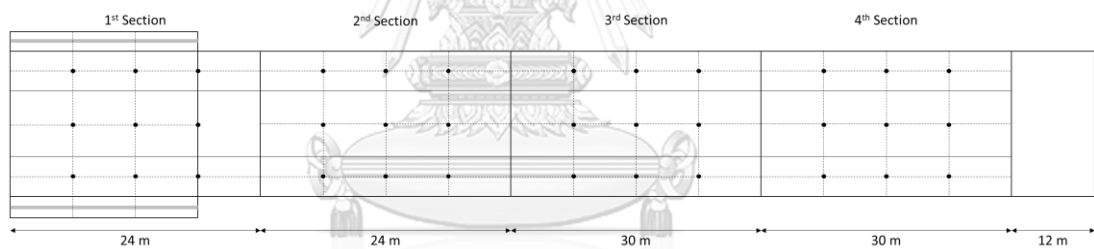


**Figure 3.2.1** Measurement locations

The experiment was conduct 2 times. The operating condition and experimental detail is shown as **Table 3.2.1**.

**Table 3.2.1** Operating condition and experimental detail

Experiment	Detail	Date and time
1	Number of chicken = 8000	11 November 2017 11.00 a.m. – 1.00 p.m.
	Age of chicken = 39 weeks	
	Number of operating fan = 8 fans	
2	Number of chicken = 7000	12 May 2018 10.00 a.m. – 12.40 p.m.
	Age of chicken = 65 weeks	
	Number of operating fan = 8 fans	

## CHAPTER 4 RESULTS AND DISCUSSIONS

### 4.1 Grid independent study

The grid independent study was conducted to determine a proper resolution of the mesh. The mesh resolution affect the accuracy of the prediction. In this study, three levels of grid resolution including coarse grid (1334000 elements), medium grid (2693000 elements) and fine grid (3700000 elements) were studied. The comparison of predicted air velocity profile from each grid resolution is shown in **Figure 4.1.1**.

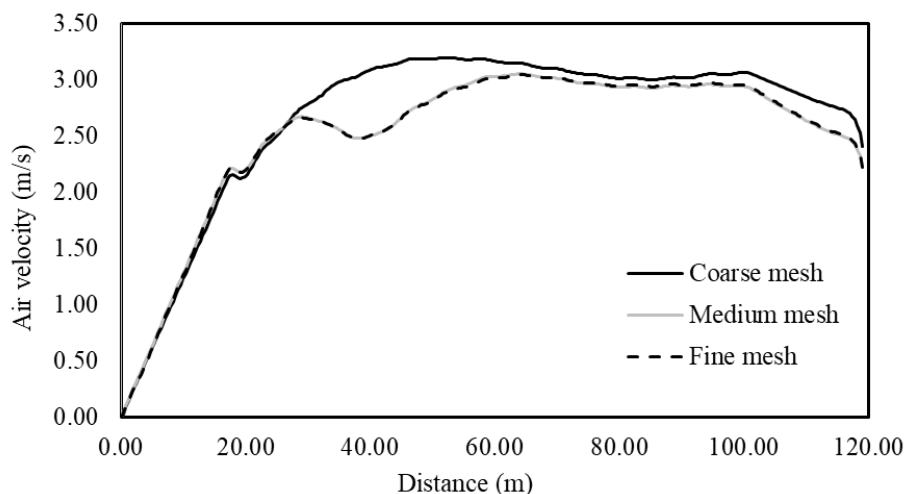


**Figure 4.1.1** Air velocity profiles at 1.5 meters height and on a vertical plane  $x = 5.1$  m from simulated using different each grid resolutions

From **Figure 4.1.1**, the results show that the medium grid is not much different from the fine grid ( $RSME_{\text{medium}} = 0.01$ ) while the coarse grid is deviated from the fine grid ( $RSME_{\text{coarse}} = 0.22$ ). Therefore the medium grid (2693000 elements) was chosen in this study.



## 4.2 Animal occupied zone modeling

In this study, an animal occupied zone (AOZ) was considered as a porous media. The pressure drop due to the resistance of the porous media can be expressed as Eq. (27). The viscous and inertial resistance coefficient can be estimated using sub-model. The sub-model can be shown as **Figure 3.1.4**. The chicken was considered as a sphere. The airflow pressure drop is occurred due to the chicken. The sub-model was applied to simulate the pressure distribution in a horizontal plane for each inlet velocity. **Figure 4.2.1** shows pressure distribution at 0.2 meter height with an inlet velocity of 2 m/s. From Eq. (27), the relation between pressure drop and inlet velocity is in the form of polynomial equation. From the relation between the average pressure drop between inlet and outlet of the AOZ and the inlet velocity of the AOZ in **Figure 4.2.2**, the inertial and viscous resistance coefficient were  $0.184 \text{ m}^{-1}$  and  $3427.78 \text{ m}^{-2}$ , respectively determined by using polynomial regression.

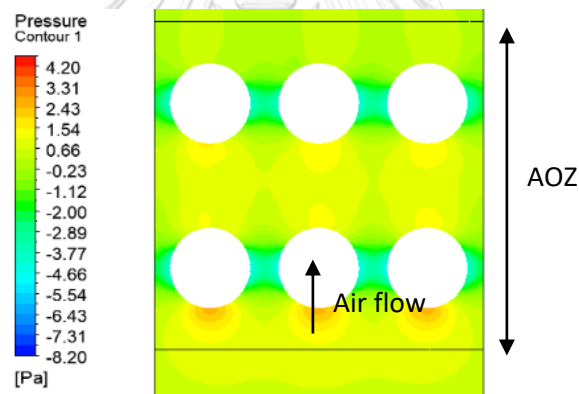
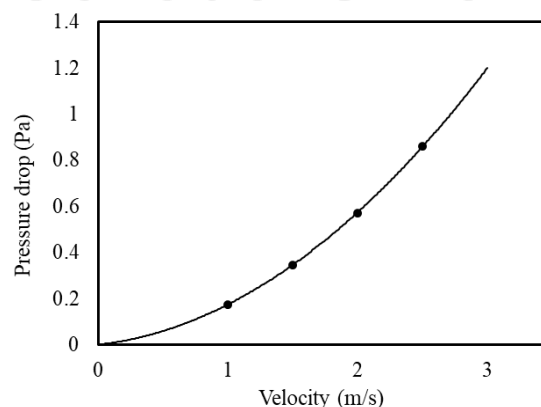


**Figure 4.2.1** Pressure distribution at 0.2 meter height for an inlet velocity 2 m/s



● : Simulation results at each inlet velocity, — : Regression line

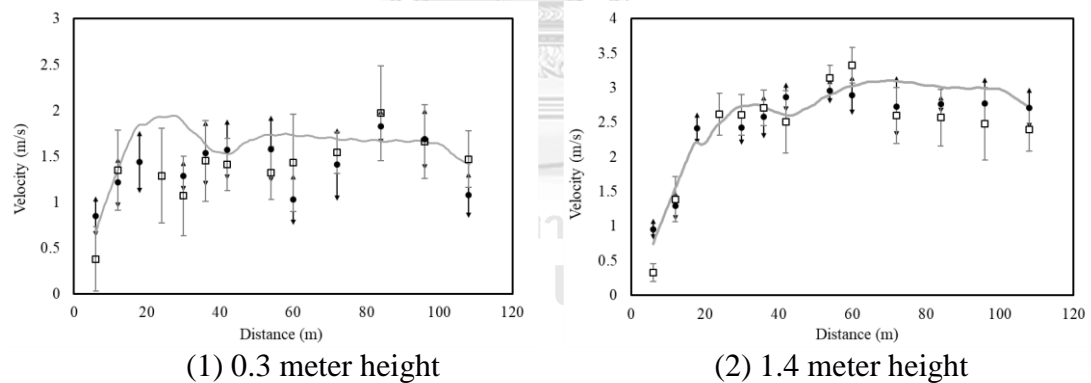
**Figure 4.2.2** Relationship between average pressure drop between inlet and outlet of the AOZ and inlet velocity of the AOZ

### 4.3 CFD validation

The validation aims to assure that the model prediction is accurate. The common method for validation is comparing between experimental results and simulated results. After the validation was conducted, the validated model can be used as a prototype for system design and modification. In this study, the simulation results which consist of air velocity, temperature and relative humidity were compared with experimental results. The validation was examined by using normalized mean square error (NMSE) calculated by Eq. (41). The model is acceptable when value of NMSE is less than 0.25 [12, 14, 16].

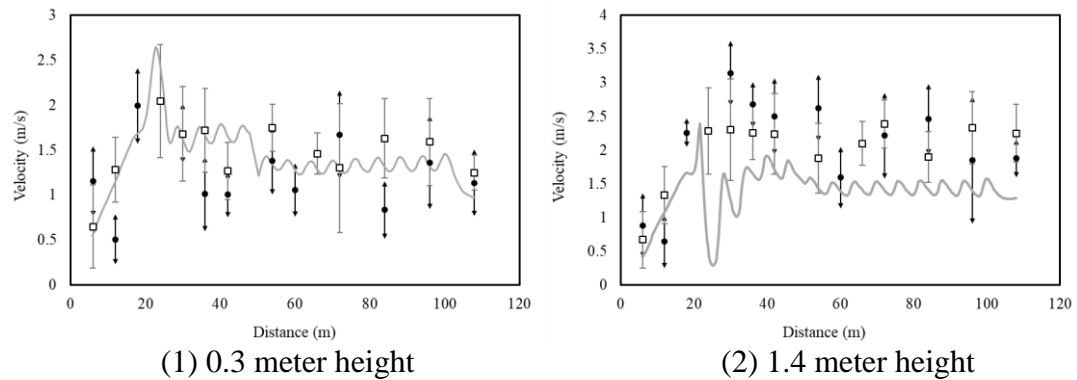
#### 4.3.1 Air velocity validation

The air velocity is one of the factors that affect the climate condition. The measurement was conducted in various location shown in Figure 3.2.1. The comparisons of simulated and measured air velocity at the middle, on the left and the right side of the chicken house were shown as **Figure 4.3.1, 4.3.2 and 4.3.3**, respectively. The values of NMSE are shown in **Table 4.3.1**.

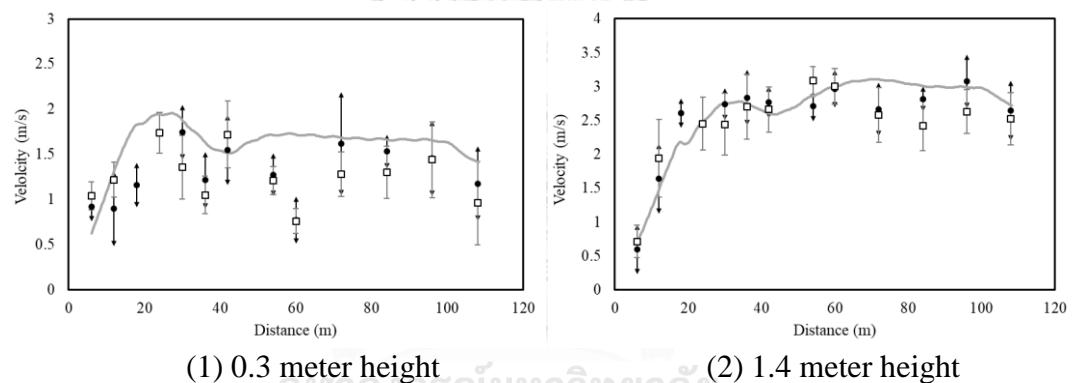


● : Data from experiment 1, □ : Data from experiment 2, — : Simulation results

**Figure 4.3.1** Comparison of simulated and measured velocity at the left side of the chicken house ( $x = 5.1$  meters) when the number of operating fans were 8 fans and the external air temperature and relative humidity were 26.5 degree Celsius and 73 percent, respectively. (Error bars represent 95 percent confidence intervals)



● : Data from experiment 1, □ : Data from experiment 2, — : Simulation results  
**Figure 4.3.2** Comparison of simulated and measured velocity at the middle of the chicken house ( $x = 0$  meter) when the number of operating fans were 8 fans and the external air temperature and relative humidity were 26.5 degree Celsius and 73 percent, respectively. (Error bars represent 95 percent confidence intervals)



● : Data from experiment 1, □ : Data from experiment 2, — : Simulation results  
**Figure 4.3.3** Comparison of simulated and measured velocity at the right side of the chicken house ( $x = -5.1$  meters) when the number of operating fans were 8 fans and the external air temperature and relative humidity were 26.5 degree Celsius and 73 percent, respectively. (Error bars represent 95 percent confidence intervals)

**Table 4.3.1** Values of normalized mean square error (NMSE) for air velocity

Location	Left		Middle		Right	
	NMSE <sup>1</sup>	NMSE <sup>2</sup>	NMSE <sup>1</sup>	NMSE <sup>2</sup>	NMSE <sup>1</sup>	NMSE <sup>2</sup>
0.3 m. height	0.05	0.06	0.11	0.03	0.09	0.12
1.4 m. height	0.01	0.02	0.27	0.28	0.01	0.02

<sup>1</sup> comparison with experimental data from measurement No. 1

<sup>2</sup> comparison with experimental data from measurement No. 2

From **Figure 4.3.1 - 4.3.3**, the reasonable agreement between simulation and experimental results were found except the simulation results at 1.4 m height and at the middle of the chicken house. These results are consistent with the values of NMSE as shown in **Table 4.3.1**. All of the NMSE values, but those at 1.4 m height and at the middle of the chicken house, are lower than 0.25, i.e., the model is acceptable. From **Figure 4.3.2** (1.4 m height), the simulation results under predict the experimental results. This is due to at 1.4 m height, the airflow is greatly influenced by the deflector. The incoming flow between the channel (i.e., between the deflector and floor) behaves like a jet flow as shown in **Figure 4.3.4**. Van Hooff et al. (2017) studied the jet flow prediction using several turbulent models. The realizable k- $\epsilon$  model provided a smaller velocity magnitude than the LES model and experiment. All of the RANS models failed to predict the maximum velocity of the jet flow correctly. The LES model could clearly better predict the velocity of the jet flow than all of the RANS models. **Figure 4.3.5** shows that the jet velocity from LES model is slightly higher than that from RANS models, i.e., standard k- $\epsilon$  model (SKE) and shear-stress transport k- $\omega$  model (SST). As a result, the predicted air velocity beneath the deflector by realizable k- $\epsilon$  model is underestimated. From Van Hoof et al. study, the suitable turbulent model for jet flow prediction is LES model [57]. However, the LES model simulation is more complicated, requires high computational demand and requires longer simulation time. In addition, RANS model can predict the overall results of the system as well as the LES model can. Furthermore, in this study the circulations due to the jet flow near the deflector are relatively far from the habitat levels of the chicken and also do not affect the overall velocity profile in the chicken house. Therefore, the realizable k- $\epsilon$  is reasonable for air velocity prediction in this study.

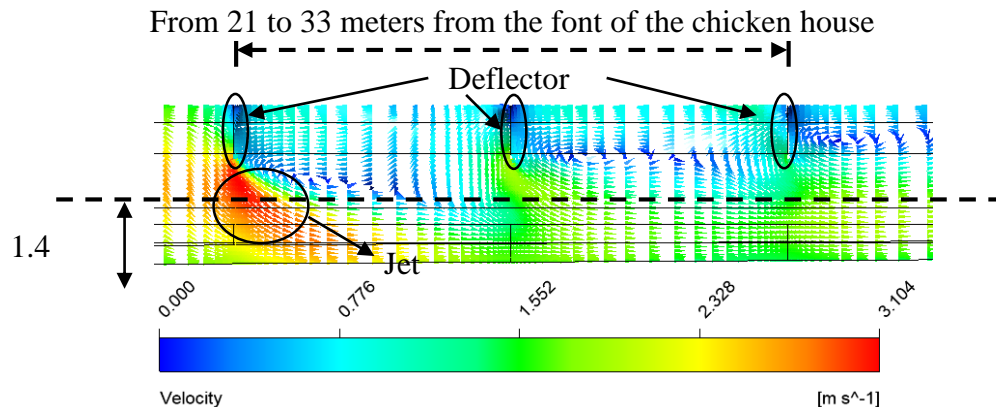


**Figure 4.3.4** Jet flow under the deflector

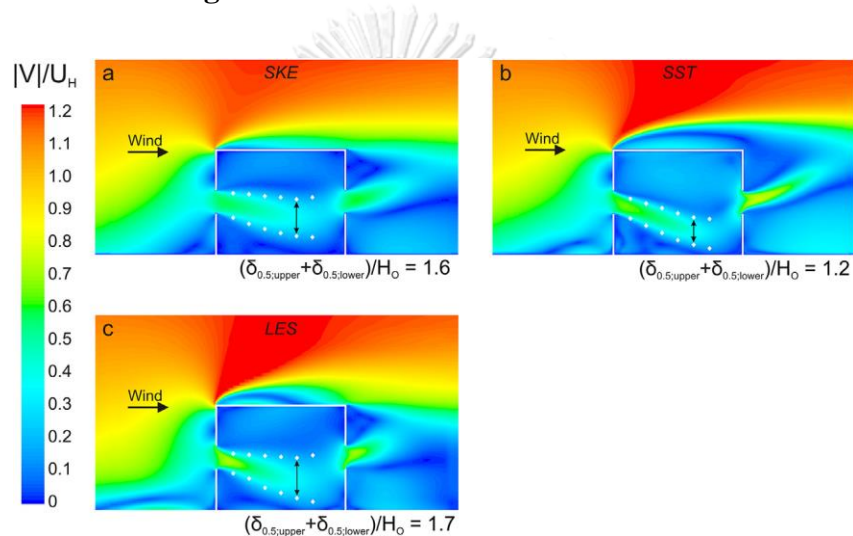


**Figure 4.3.5** Predicted velocity distribution from RANS model (SKE and SST) and LES model studied by Van Hoof et al. [57]

#### 4.3.2 Air temperature and relative humidity validation

The comparison of simulated and measured temperature at the middle, on the left and on the right side are shown in **Figure 4.3.6, 4.3.7 and 4.3.8**, respectively. **Figure 4.3.9 – 4.3.11** show the comparison of simulated and measured relative humidity at middle, on the left and on the right side. **Table 4.3.2** shows the value of NMSE for air temperature and relative humidity.

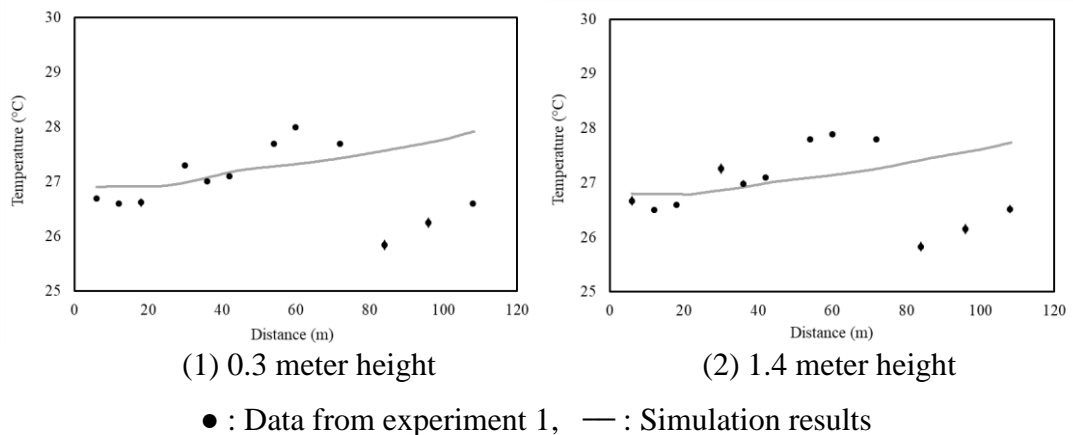


**Figure 4.3.6** Comparison of simulated and measured temperature at the left side of the chicken house ( $x = 5.1$  meters) when the number of operating fans were 8 fans and the external air temperature and relative humidity were 26.5 degree Celsius and 73 percent, respectively. (Error bars represent 95 percent confidence intervals)

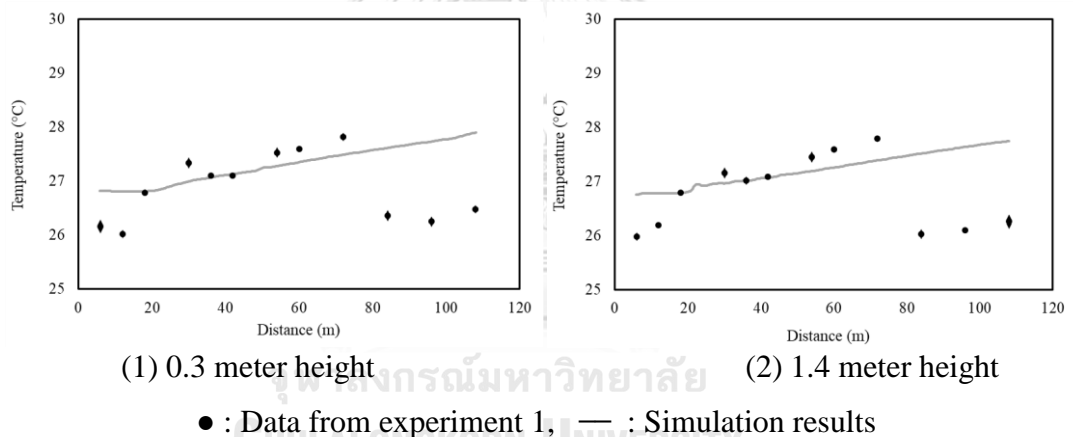


**Figure 4.3.7** Comparison of simulated and measured temperature at the middle of the chicken house ( $x = 0$  meter) when the number of operating fans were 8 fans and the external air temperature and relative humidity were 26.5 degree Celsius and 73 percent, respectively. (Error bars represent 95 percent confidence intervals)

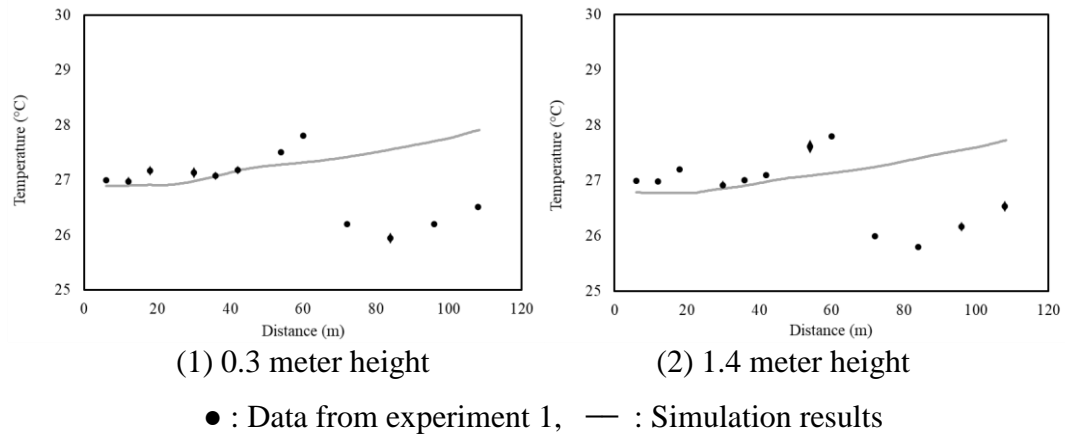


**Figure 4.3.8** Comparison of simulated and measured temperature at the right side of the chicken house ( $x = -5.1$  meters) when the number of operating fans were 8 fans and the external air temperature and relative humidity were 26.5 degree Celsius and 73 percent, respectively. (Error bars represent 95 percent confidence intervals)

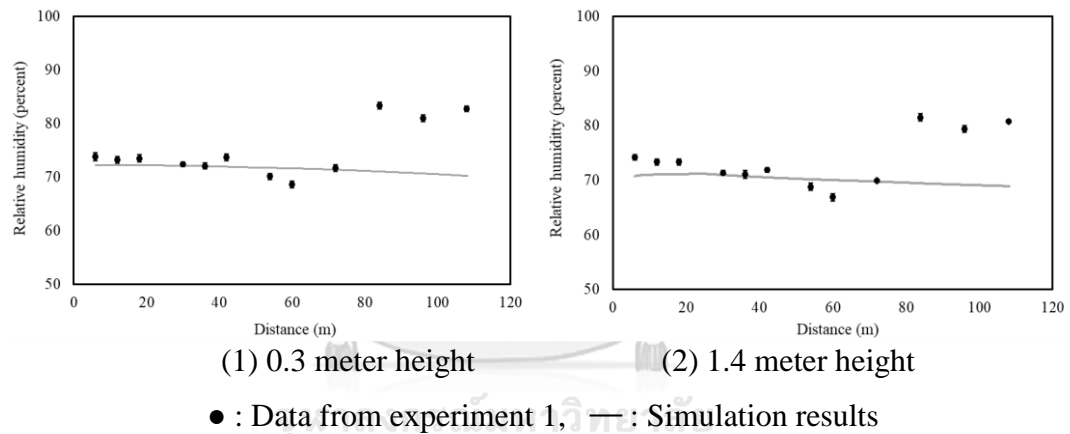
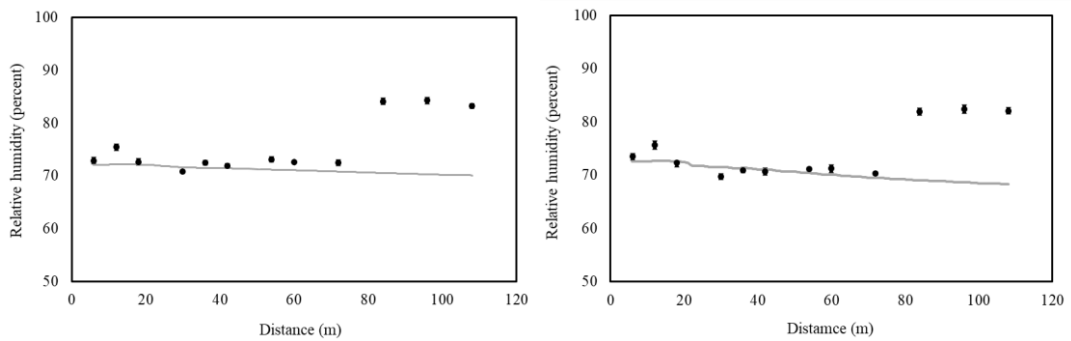


**Figure 4.3.9** Comparison of simulated and measured relative humidity at the left side of the house ( $x = 5.1$  meters) when the number of operating fans were 8 fans and the external air temperature and relative humidity were 26.5 degree Celsius and 73 percent, respectively. (Error bars represent 95 percent confidence intervals)

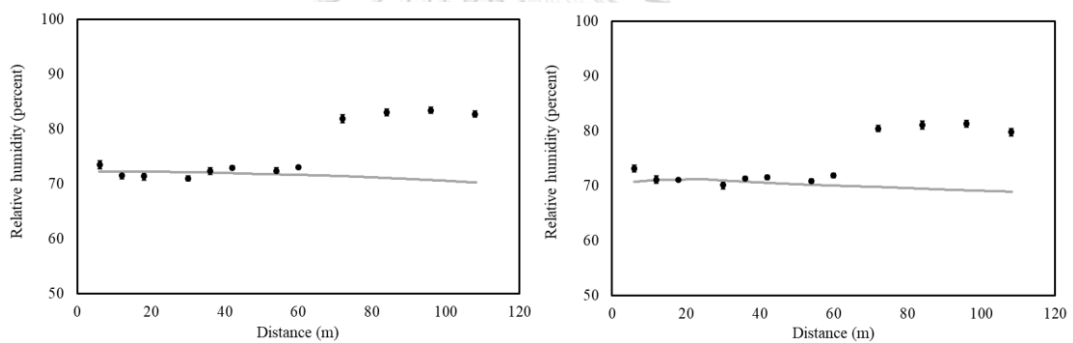


(1) 0.3 meter height

(2) 1.4 meter height

● : Data from experiment 1, — : Simulation results

**Figure 4.3.10** Comparison of simulated and measured relative humidity at the middle of the house ( $x = 0$  meter) when the number of operating fans were 8 fans and the external air temperature and relative humidity were 26.5 degree Celsius and 73 percent, respectively. (Error bars represent 95 percent confidence intervals)



(1) 0.3 meter height

(2) 1.4 meter height

● : Data from experiment 1, — : Simulation results

**Figure 4.3.11** Comparison of simulated and measured relative humidity at the right side of the house ( $x = -5.1$  meters) when the number of operating fans were 8 fans and the external air temperature and relative humidity were 26.5 degree Celsius and 73 percent, respectively. (Error bars represent 95 percent confidence intervals)



**Table 4.3.2** Values of normalized mean square error (NMSE) for temperature (T) and relative humidity (RH)

Location	Left		Middle		Right	
	T	RH	T	RH	T	RH
0.3 m height	4.32E-04	1.58E-04	4.98E-04	2.10E-04	1.77E-04	6.59E-05
1.4 m height	8.27E-04	2.54E-04	3.90E-04	1.97E-04	2.48E-04	1.70E-04

From **Figure 4.3.6 – 4.3.11**, the model is capable of predicting temperature and relative humidity accurately. The value of NMSE for temperature and relative humidity at all location are lower than 0.25 which implied that the model is acceptable. Note that the last 3 – 4 data points in **Figure 4.3.6 – 4.3.11**, the temperature decreases and the relative humidity increases because the evaporative cooling pad was operated during the experiment. Therefore, the NMSE calculations were not performed for these measurement disturbance.

#### 4.4 CFD simulation

The validated model was applied to study the climate condition (i.e. air velocity, temperature and relative humidity) inside the chicken house. Moreover, the effective temperature at the chicken level was investigated to indicate the suitability of the climate for the chicken.

##### 4.4.1 Internal air velocity distribution

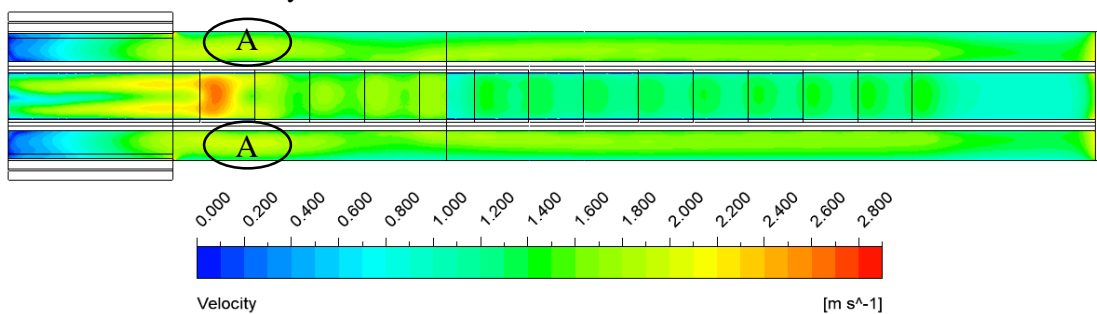


**Figure 4.4.1** Air velocity at chicken level when the number of operating fans were 8 fans and the external air temperature and relative humidity were 26.5 degree Celsius and 73 percent, respectively.

**Figure 4.4.1** shows air velocity at chicken level (0.3 m height from the floor and the slat). The air velocity gradually increases from the front to the end of the chicken house due to influence of the exhaust fans at the end of the chicken house. **Figure 4.4.2** shows the airflow direction influenced by the inlet deflector. The inlet deflector forces the air flow toward the roof. Then, the air circulates to the floor. This circulation causes swirling flow at the middle of the house and causes some of the air flow into the side of the house. Therefore, the inlet deflector installation can mitigate the dead zone where the air flow changes direction as shown in area A in **Figure 4.4.1**.

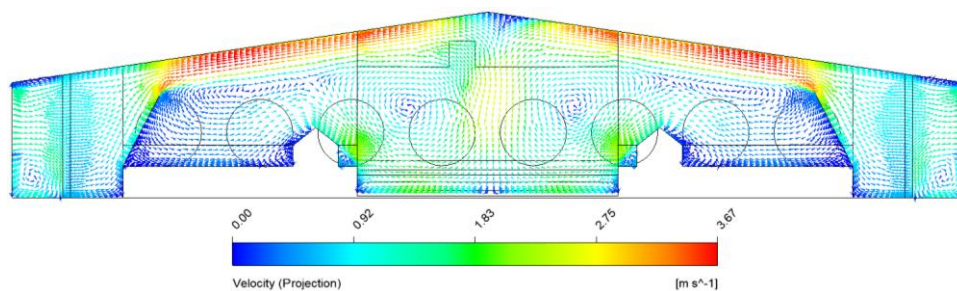


**Figure 4.4.2** Airflow direction influenced by inlet deflector in a vertical plane  $z = 9$  m when the number of operating fans were 8 fans and the external air temperature and relative humidity were 26.5 degree Celsius and 73 percent, respectively.

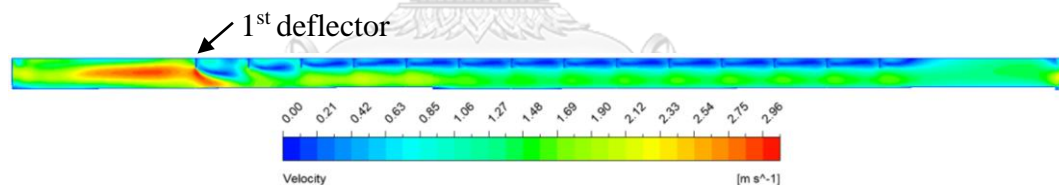


**Figure 4.4.3** Air velocity influenced by deflector in a vertical plane at  $x = 0$  when the number of operating fans were 8 fans and the external air temperature and relative humidity were 26.5 degree Celsius and 73 percent, respectively.

The effect of deflector can be shown in **Figure 4.4.3**. The air which flows through the middle of the house hits the first deflector at high velocity. Thus, the air flows toward the floor with high velocity and impacts the chicken in this area. In addition, the deflector disperses the incoming air toward the sides of the house. The air flow direction at the first deflector can be shown in **Figure 4.4.4**. The effect of the latter deflector can be observed from the fluctuation of the velocity shown in **Figure 4.4.3**. At the rear end of the house, the air velocity magnitude which hits the deflector is lower than the initial deflector. **Figure 4.4.5** shows that the air is dispersed toward the chicken occupied zone with low velocity magnitude due to the deflector. Thus, the air velocity

at the chicken occupied zone is low too. From **Figure 4.4.1**, the air velocity at the sides of the house (from area A to the rear end of the chicken house) is quite stable because the effect of the deflector is not strong. The air velocity which hit the deflectors after the first and second deflector is low so that the air is dispersed toward the sides of the chicken house is low. This can be observed from the color represented the air velocity. The color at the sides of the house does not much change along the length of the chicken house.

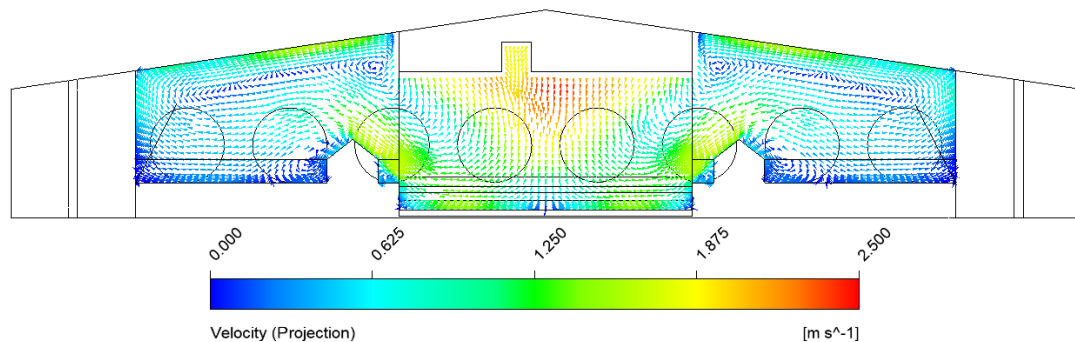


**Figure 4.4.4** Airflow direction influenced by deflector at a vertical plane  $z = 21$  meters when the number of operating fans were 8 fans and the external air temperature and relative humidity were 26.5 degree Celsius and 73 percent, respectively.

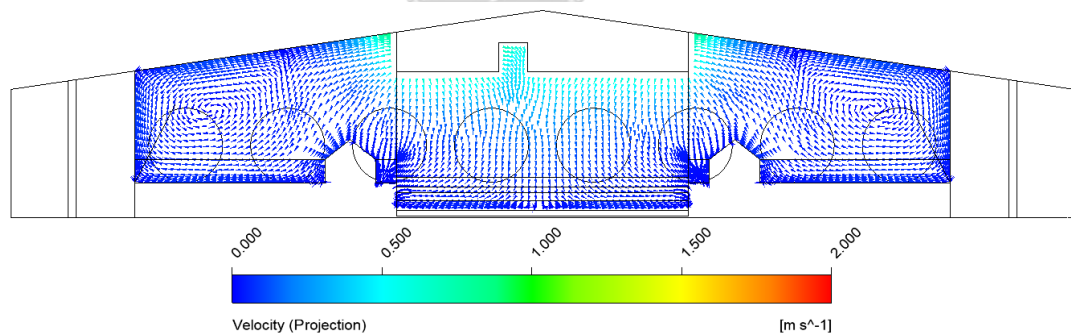


**Figure 4.4.5** Airflow direction influenced by deflector at a vertical plane  $z = 81$  meters when the number of operating fans were 8 fans and the external air temperature and relative humidity were 26.5 degree Celsius and 73 percent, respectively.

#### 4.4.2 Internal air temperature and relative humidity distribution

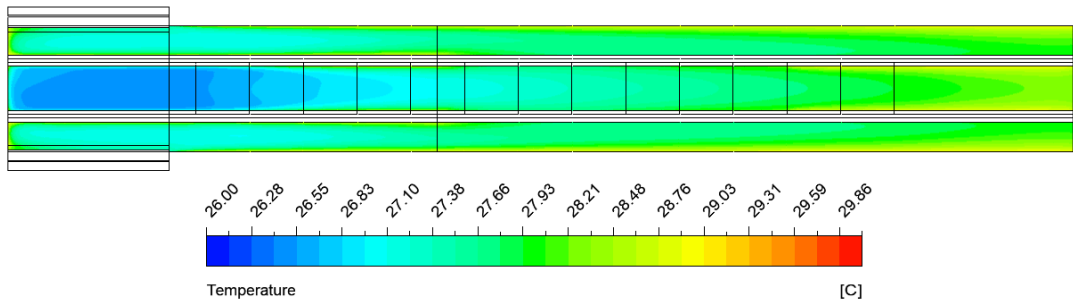


**Figure 4.4.6** Air temperature at chicken level (0.3 meter height) when the number of operating fans were 8 fans and the external air temperature and relative humidity were 26.5 degree Celsius and 73 percent, respectively.

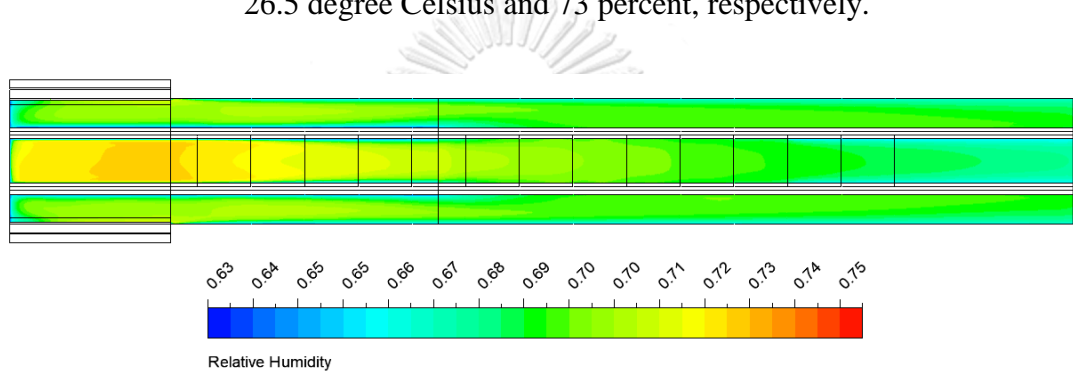


**Figure 4.4.7** Relative humidity at chicken level (0.3 meter height) when the number of operating fans were 8 fans and the external air temperature and relative humidity were 26.5 degree Celsius and 73 percent, respectively.

The air temperature distribution at chicken level is shown in **Figure 4.4.6**. The air temperature increases along the length of the house because the airflow induces the heat convection which carries the emitted heat from the chicken to the outlet. Moreover, the heat transfer from the wall and roof also increases the air temperature. **Figure 4.4.7** shows the relative humidity distribution at chicken level. The relative humidity slightly decreases from the front to the end of the chicken house although there is emitted moisture from the chicken and litter. As the result of the increase in temperature, the air can hold higher amount of water vapor. Thus, the relative humidity decreases, i.e., further from being saturated, along the length of the house.

#### 4.4.3 Effective temperature at the chicken level

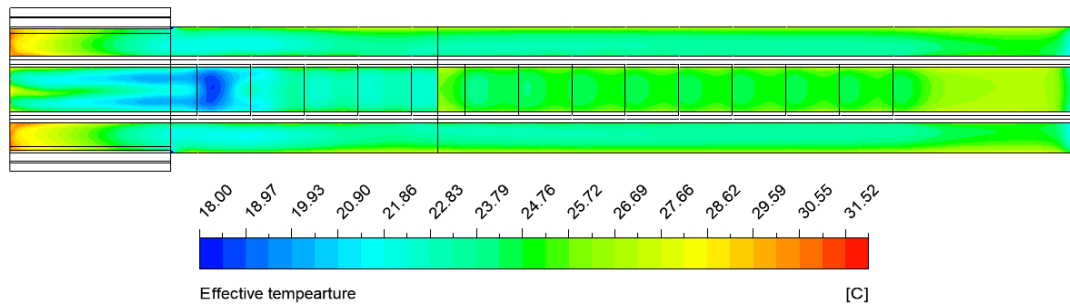


**Figure 4.4.8** Effective temperature at chicken level (0.3 meter height) when the number of operating fans were 8 fans and the external air temperature and relative humidity were 26.5 degree Celsius and 73 percent, respectively.

The effective temperature is an indicator of the climate condition. **Figure 4.4.8** shows the effective temperature at chicken level which is calculated from air velocity, temperature and relative humidity. The optimal effective temperature for chicken during egg-producing ages is at  $21 \pm 3$  degree Celsius [33]. The simulation result shows that the effective temperature at the inlet (24-28 degree Celsius) is higher than optimal range. This is due to low air velocity near the inlet. The air velocity beneath the first deflector is very high so that the effective temperature in this area is the lowest. In addition, the simulation results were investigated to determine the uniformity of the climate inside the chicken house. From the figure, the effective temperature at the middle of the house is relatively higher than the sides of the house because of low air velocity. This is due to the air which hits the deflector with low velocity so that the air is dispersed to the chicken occupied zone with low velocity too. At the end of the house, the effective temperature is high due to the increase in temperature.

After the validation, the model was applied to develop an operational guideline to maintain a favorable climate for the chicken when the external climate changes at various condition throughout a year period. Moreover, the validated model was used to guide the modification of the chicken house in order to improve the climate inside the chicken house when the external climate is at extreme conditions.

#### 4.5 Operating condition guideline

Normally, the aim of the operation in the chicken house is to maintain the climate condition within chicken thermo neutral zone [8]. The operation consists of 1) adjust the number of working exhaust fans to increase or decrease air velocity and 2) turn on the evaporative cooling pad to decrease the inlet air temperature. The operation depends to the internal climate condition which is varied mainly due to the external climate condition, i.e., the environment. **Figure 4.5.1** shows a scatter plot of temperature and relative humidity change during year 2015 and 2017 at Pak Chong district, Nakhon Ratchasima province, Thailand [55, 56]. The data were collected 8 times (e.g. 1.00 a.m., 4.00 a.m., 7.00 a.m., 10.00 a.m., 1.00 p.m., 4.00 p.m., 7.00 p.m. and 10.00 p.m.) to sufficiently keep track of weather changes on each day. In addition, during year 2015, the El Nino phenomena occurred and caused the temperature during this year trend to higher than other years [58]. Thus, the weather data of this year were also considered to determine possible extreme weather condition for the chicken

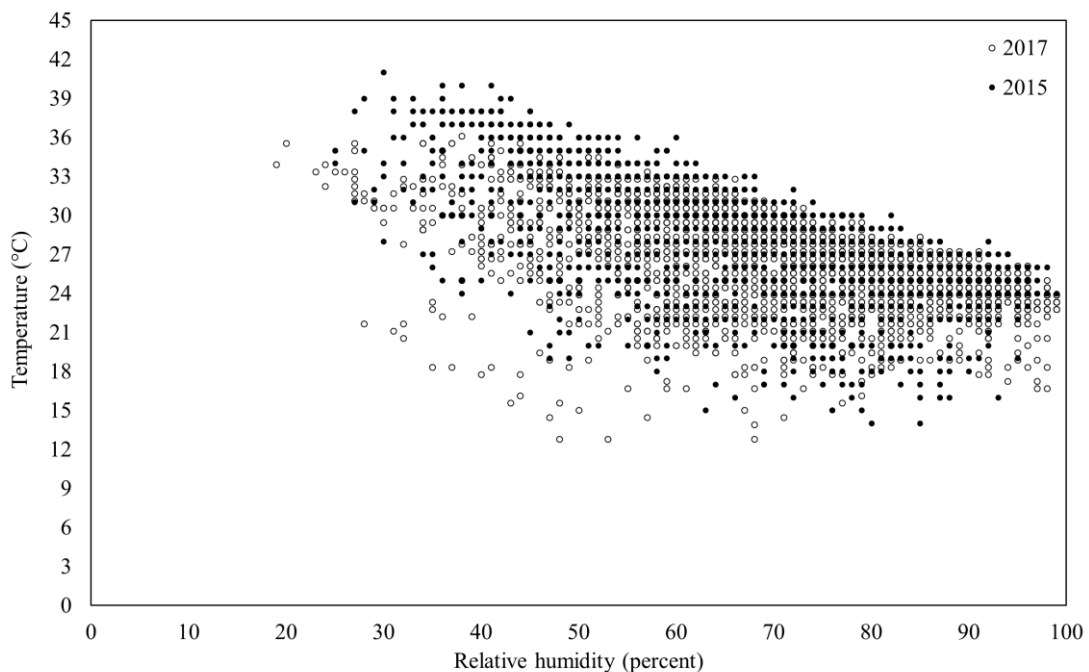


**Figure 4.5.1** Temperature and relative humidity conditions of the weather during 2015 and 2017 at Pak Chong district, Nakhon Ratchasima province, Thailand [55, 56].

The chicken thermal stress can be occurred when the temperature of air from the environment is higher than 30 degree Celsius [8]. Generally, the temperature at center of the chicken house is higher than that at the front by 1 degree Celsius and lower than that at the end of the chicken house by 1 degree Celsius [59] In other words, the temperature difference between the front (lower temperature) and the end (higher temperature) of the chicken house is approximately 2 degree Celsius. In order to prevent the temperature in the house from getting higher than thermo neutral zone, the evaporative cooling pad system must be turned on when the external air temperature is higher than 28 degree Celsius [59].

The validated model was applied to simulate interior climates by setting inlet boundary condition based on the weather data from **Figure 4.5.1**. The simulation results were investigated to determine the number of fans which cause the effective temperature at chicken level to be within the optimal range. **Figure 4.5.2** shows the operational guideline which indicates the suitable number of fans and operational of evaporative cooling pad system. The example of operational guideline consideration is described in **Appendix C**. However, at air temperature of higher than 39 degree Celsius and relative humidity of about 30 – 40 percent, the chicken house of original design cannot provide the suitable effective temperature at the chicken level even with maximum number of fans (12 fans) and evaporative cooling pad were turned on (detail in **section 4.6**). Therefore, it is needed to study the chicken house modification to achieve the optimal effective temperature for chicken welfare.



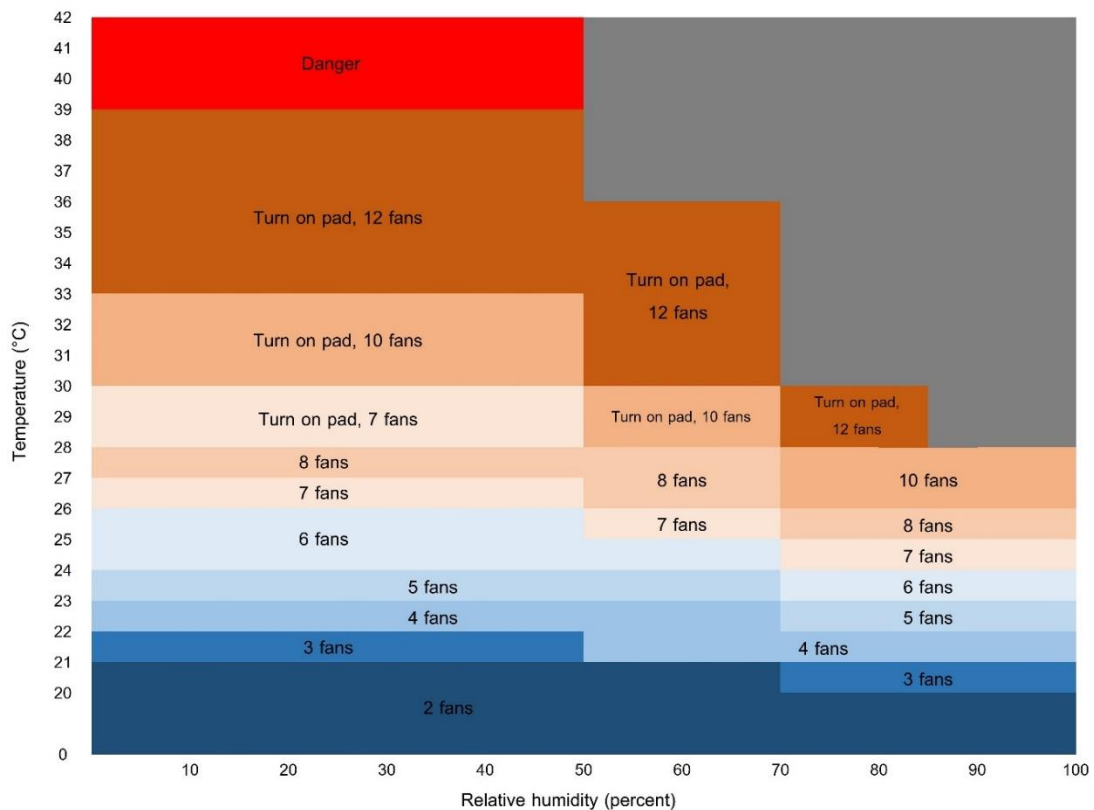


**Figure 4.5.2** Operational guideline which indicates the suitable number of fans and operational of evaporative cooling pad system for maintain the effective temperature at chicken level to be within the optimal range

#### 4.6 Chicken house simulation in extreme climate condition.

The design of the chicken house was modified in order to maintain suitable interior climate condition even in extreme environment. Thus, the capability of the original design and adjustable operating parameters, such as exhaust fans and evaporative cooling pad, in handling extreme weathers (based on the weather data in **Figure 4.5.1**) was investigated. From the **Figure 4.5.1**, the extreme temperature and relative humidity are at 41 degree Celsius and 40 percent, respectively. With 85 percent evaporative cooling pad efficiency, the incoming air temperature and relative humidity from the pad are at 30.5 degree Celsius and 88 percent, respectively. At this condition, the roof temperature, estimated by extrapolation from the measurement, is at 50 degree Celsius. With the maximum number of exhaust fans (i.e., 12 fans) and evaporative cooling pad in operation, the effective temperature of the air at chicken level in the chicken house with original design is shown as **Figure 4.6.1**.



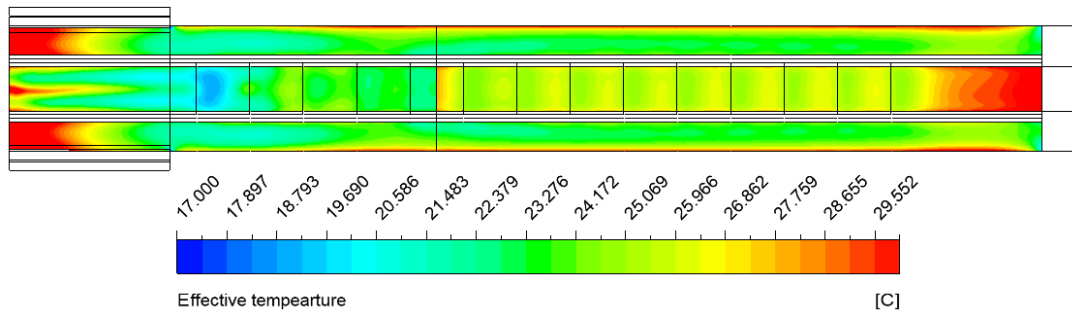


**Figure 4.6.1** Effective temperature at chicken level when evaporative cooling pad and 12 exhaust fans are operated. (Note: external temperature and relative humidity are 41 degree Celsius and 40 percent, respectively.)

From **Figure 4.6.1**, the effective temperature at the front of the chicken house is at 28 to 30 degree Celsius and the effective temperature from the center to the end of the chicken house is gradually increases from 24 to 30 degree Celsius. This implies that even with maximum number of fans and evaporative cooling pad, the original design of the chicken house cannot maintain the effective temperature within the optimal range. The factors that potentially cause the effective temperature to exceed the optimal range are as following:

- 1.) The heat transferred from the roof

From the simulation in **Figure 4.6.2**, the air temperature at the chicken level increases approximately 6 degree Celsius from the front end to the end end of the house. The increase in temperature is due to two factors which are the heat emitted from the chicken and the heat transferred from the roof. **Figure 4.6.3** shows the gradient of temperature on a vertical plane  $x = 0$ . The gradient or difference between the temperature at the roof and the bulk air flow causes the heat transfer from the roof into the chicken house. The heat transfer rate from the roof into the chicken house is at 420 kW

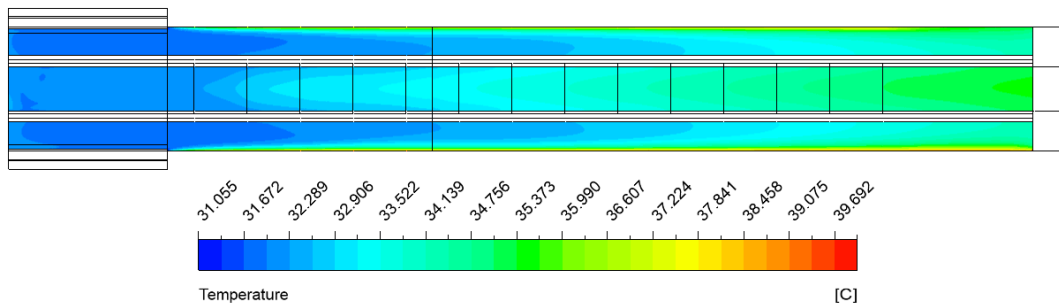


**Figure 4.6.2** Air temperature at chicken level when evaporative cooling pad and 12 exhaust fans are operated.

(Note: external temperature and relative humidity are 41 degree Celsius and 40 percent, respectively.)

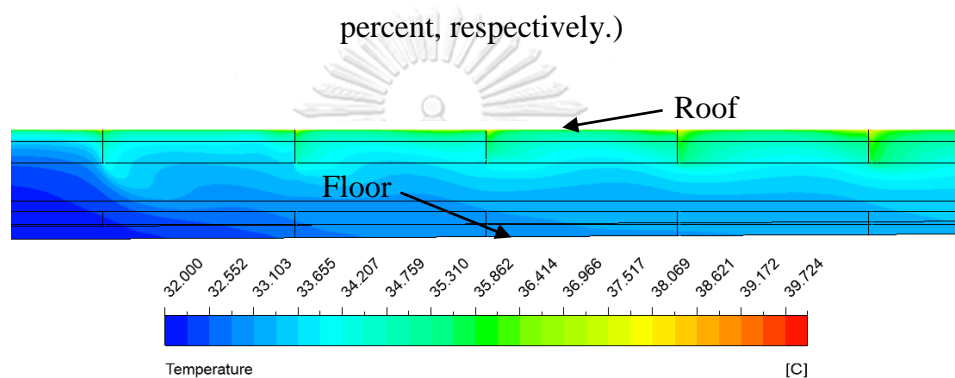


**Figure 4.6.3** Temperature gradient on a vertical plane  $x = 0$  when evaporative cooling pad and 12 exhaust fans are operated.

(Note: external temperature and relative humidity are 41 degree Celsius and 40 percent, respectively.)

- 2.) At this operating condition (i.e., maximum fan number) and original design of the chicken house, the air blown through chicken occupied zone was still not at sufficient velocity. **Figure 4.6.4** shows the air velocity at chicken level. The air velocity magnitude is approximately 2.2 – 2.7 meters per second. If higher velocity can be achieved, the heat convection from the chicken to the outlet can be increased and the temperature is reduced.

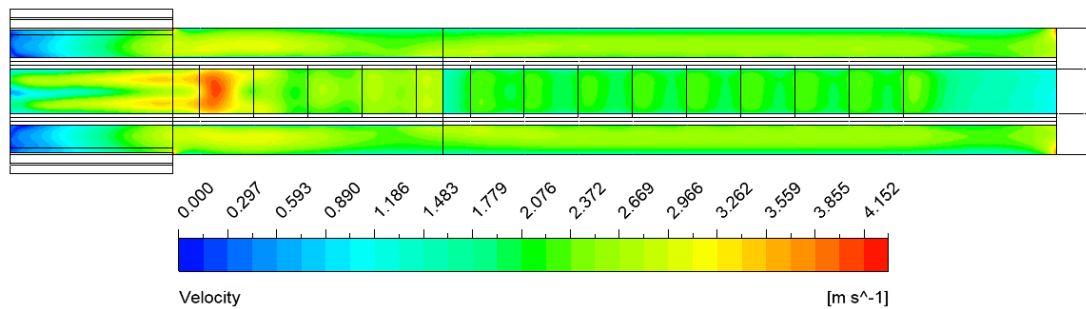


**Figure 4.6.4** Air velocity at chicken level when evaporative cooling pad and 12 exhausted fans operated.

(Note: external temperature and relative humidity are 41 degree Celsius and 40 percent, respectively.)

## 4.7 Modification of the chicken house

From **section 4.6** the factors that contribute to unsuitable climates inside the chicken house are high heat transfer rate from the roof into the chicken house and insufficient air flow rate through the chicken occupied zone. The modification of the chicken house, which was aimed at maintaining favorable interior climates can be described as follows.

### 4.7.1 Thermal insulation

One of the methods for preventing the heat transfer from the roof is thermal insulation. Thus, the validated model was applied to simulate the chicken house with thermal insulation. The modification of the chicken house can be expressed as shown in **Figure 4.7.1**. The thermal insulator was installed under the roof. Two thicknesses of insulation (i.e. 25 and 50 mm) were considered in this study. The insulator properties are referred from SCG thermal insulation for roof (Super Cool-G) [60]. Thermal conductivity and density were 0.035 W/m.K and 24 kg/m<sup>3</sup>, respectively.

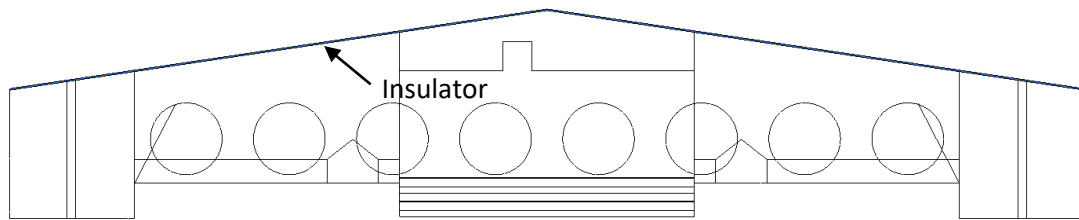


**Figure 4.7.1** Installed thermal insulator under the roof

The comparison of temperature at chicken level between modified and original chicken house can be shown as **Figure 4.7.2**.

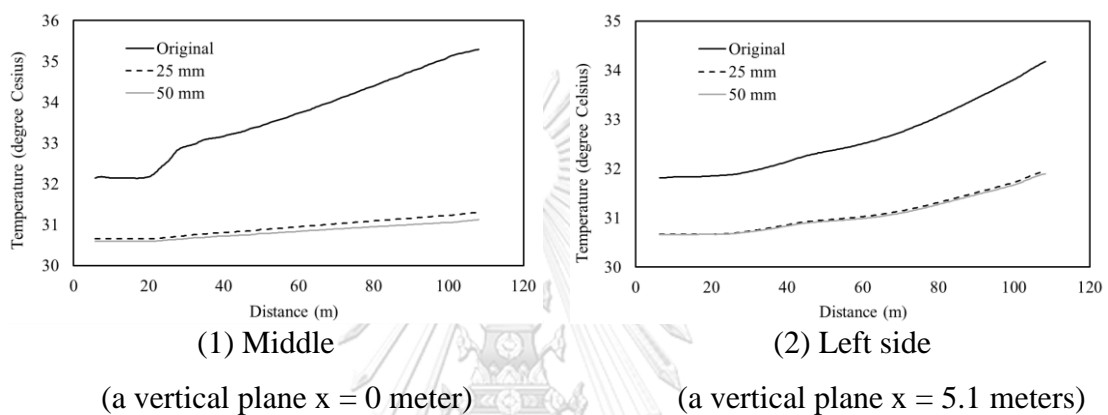


**Figure 4.7.2** Comparison of temperature at chicken level in the modified (i.e., add insulation) and original chicken house when evaporative cooling pad and 12 exhausted fans operated.

(Note: external temperature and relative humidity are 41 degree Celsius and 40 percent, respectively.)

From the results, the thermal insulation can decrease the temperature by 1 degree Celsius at the front end of the house and 4 degree Celsius at the end of the house. Moreover, it also results in the difference of temperature between at the front and the rear ends by approximately 1 degree Celsius (versus 3 degree Celsius in the original design without the insulation). This implies that the thermal insulation also helps improve the uniformity of temperature. However, the decrease in temperature is not significantly different between two thicknesses, i.e., 25 and 50 mm insulators. In conclusion, installation of 25 mm thermal insulator can effectively reduce the heat transfer from the roof into the chicken house. The heat transfer rate from the roof into the chicken house is decreased from 420.3 kW to 42.4 kW (90 percent) after the insulator installation. Air temperature distribution after insulator is installed in the

chicken house with original design can be shown in **Figure 4.7.3**. The figure shows a good uniformity of temperature profile. The effective temperature at chicken level after insulator installation is shown in **Figure 4.7.4**. The effective temperature is decreased compared to that in the original design of chicken house (**Figure 4.6.4**). The effective temperature at the sides of the chicken house is decreased from 24 degree Celsius to 21-22 degree Celsius after thermal insulator installation. However, the effective temperature at the middle of the house is decreased from 26 degree Celsius to 24-25 degree Celsius which is still higher than optimal range.

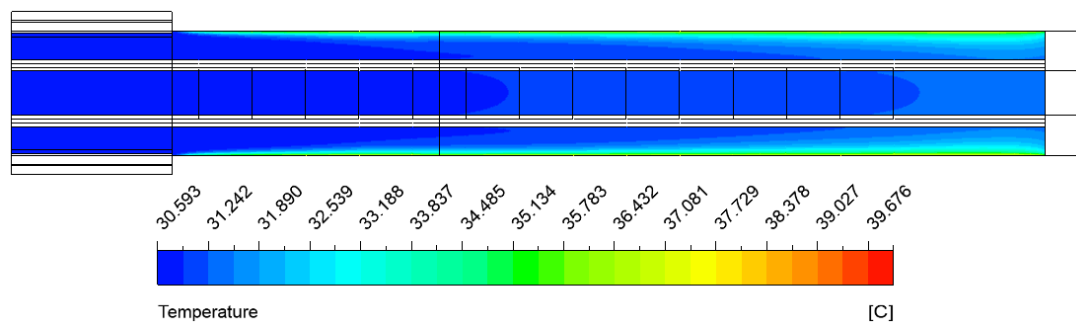


**Figure 4.7.3** Temperature distribution at chicken level after insulator is installed when evaporative cooling pad and 12 exhausted fans operated.

(Note: external temperature and relative humidity are 41 degree Celsius and 40 percent, respectively.)

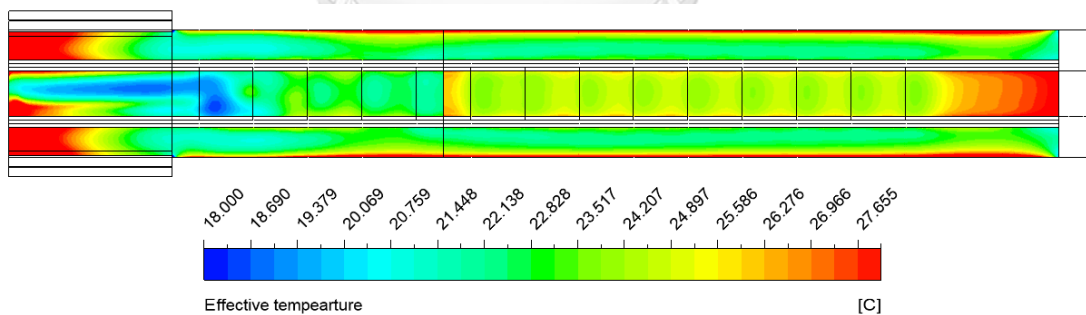


**Figure 4.7.4** Effective temperature distribution after insulator installed when evaporative cooling pad and 12 exhausted fans operated.

(Note: external temperature and relative humidity are 41 degree Celsius and 40 percent, respectively.)

#### 4.7.2 Deflector modification

Increasing the air velocity is a common technique for reducing temperature to improve chicken welfare. The aim of deflector installation is to decrease the cross-sectional area of the airflow inside the chicken house to increase the air velocity. Moreover, without the deflector the air is mainly flow along the middle of the chicken house. The deflector helps disperse the air to the sides of the chicken house.

In this study, the original deflector cannot provide sufficient air velocity (see **Figure 4.6.4**) to achieve the optimal range of effective temperature when the outside temperature is very high and the maximum number of the exhaust fans are operated. It is due to exceeded cross sectional area of the airflow. Moreover, at the middle of the rear section of the chicken house is slightly lower than the sides of the house. Because the deflector enhances the air dispersion to the sides of the chicken house, the air at the middle of the rear section of chicken house is at low velocity. The airflow at the rear end of the house hits the deflector at low velocity. Thus, the amount of air which is deflected to the chicken occupied zone is low too. Therefore, it is needed to modify the deflector for improving the airflow at the chicken level. The original deflector was modified into 2 types, i.e., broad and long deflectors, as shown in **Figure 4.7.5 and Figure 4.7.6**, respectively. The broad deflector extends the width of the original deflector from 2.5 meters from the center to 6.5 meters from the center. The aims of the extension were to decrease the cross sectional area and to deflect the air to the chicken occupied zone at both sides and middle of the chicken house. The long deflector lengthen the length of the original deflector. The length between the lower edge of the deflector and the floor is decreased from 2.5 meters to 2.2 meters. The idea of modification is that when the lower edge of the deflector is moved down, the amount of air dispersion from the deflector should be increased at both sides and the middle of the chicken house. The validated CFD model was applied to simulate the air velocity distribution due to the modified deflector in the chicken house with original design.

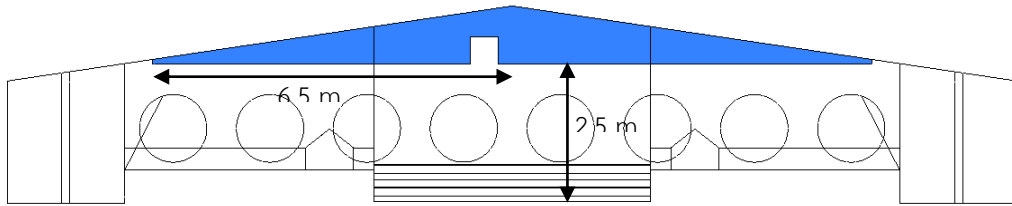


**Figure 4.7.5** Broad deflector

(The width of the deflector is extended from 2.5 meters to 6.5 meters)

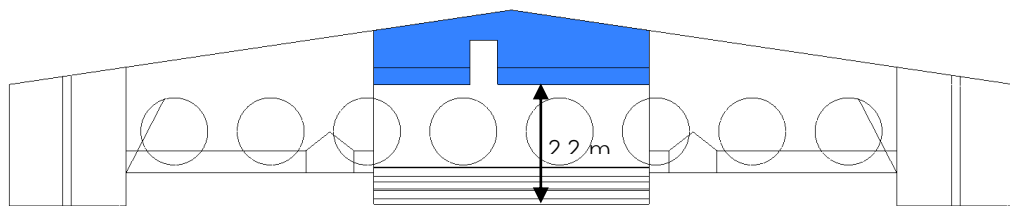


**Figure 4.7.6** Long deflector

(The length from the floor to the lower edge of the deflector is decreased from 2.5 meters to 2.2 meters)

The comparison of simulated air velocity at chicken level, when the original deflectors, broad deflector and long deflector were applied, is presented as **Figure 4.7.7**. In addition, **Figure 4.7.8** and **Figure 4.7.9** show the simulated contour of air velocity at chicken level in the chicken house with broad and long deflectors, respectively.

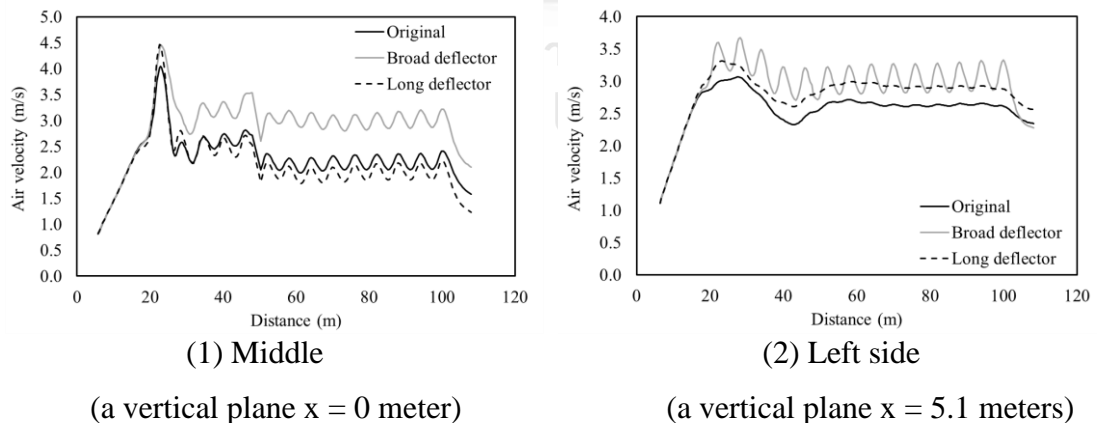


**Figure 4.7.7** Comparison of air velocity at chicken level from original deflector, broad and long deflector when evaporative cooling pad and 12 exhausted fans operated.

(Note: external temperature and relative humidity are 41 degree Celsius and 40 percent, respectively.)

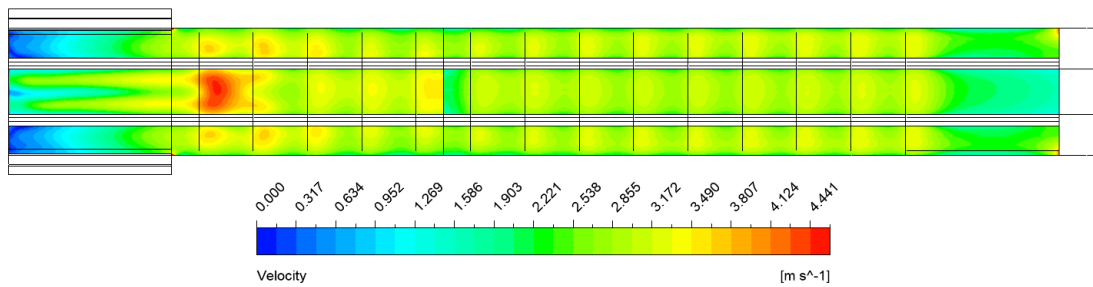


**Figure 4.7.8** Contour of air velocity on a horizontal plane at chicken level in the chicken house with broad deflectors when evaporative cooling pad and 12 exhausted fans operated.

(Note: external temperature and relative humidity are 41 degree Celsius and 40 percent, respectively.)

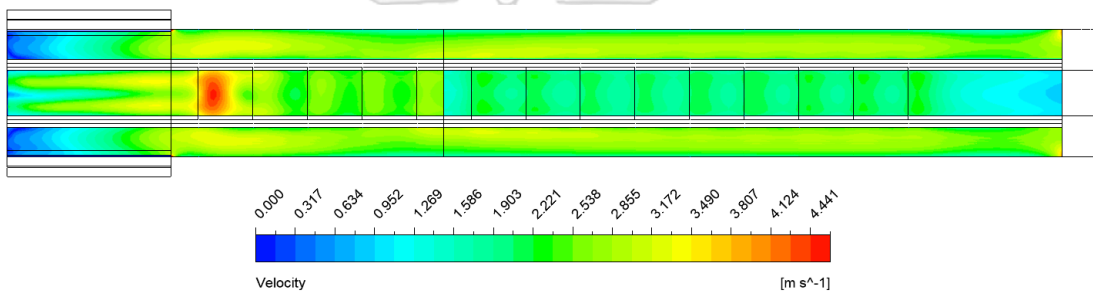


**Figure 4.7.9** Contour of air velocity on a horizontal plane at chicken level in the chicken house with long deflectors when evaporative cooling pad and 12 exhausted fans operated.

(Note: external temperature and relative humidity are 41 degree Celsius and 40 percent, respectively.)

From the results, the broad deflector significantly increases air velocity along the middle and the sides of the house as shown in **Figure 4.7.8**. It is because the broad deflector decreases the cross sectional area of airflow at both middle and sides of the house. In addition, broad deflector results in similar velocity magnitude ( $\sim 3$  m/s) along both the middle and the sides of the house. The reason is that when the air hits the deflector, the air is deflected to the chicken occupied zone at both the middle and the sides of the chicken house as shown in **Figure 4.7.10**. This implies that it enhances the uniformity of air velocity in the chicken house except the front and rear end of the house and near the first two deflector as illustrated in **Figure 4.7.8**. In addition, from **Figure 4.6.4** and **Figure 4.7.9**, the original deflector and long deflector result in similar air velocity distributions. However, the air velocity along the middle of the chicken house



with longer deflector is slightly lower than that with the original deflector. This is in contrast with the result of air velocity profile along the side of the chicken house, i.e., the long deflector results in higher air velocity than the original deflector. This is because the long deflector has more vertical area than original deflector. The long deflector enhance the air dispersion to the sides of the chicken house but does not improve the air dispersion at the middle of the chicken house. This can be illustrated in **Figure 4.7.11**.

From **Figure 4.7.8** and **Figure 4.7.9**, it can observe that there is the wavy velocity profile at the deflector area. The wavy velocity profile is happened due to the influence of the deflector. When the air hits the deflector, it causes the air velocity beneath the deflector increase. After that, the air velocity is decreased due to the increasing in cross sectional area of airflow. This is in contrast with the velocity profile at the area without the deflector (i.e., the sides of the chicken house in **Figure 4.7.9**). At this area the velocity profile is smooth because it is not affected by the influence of the deflector.

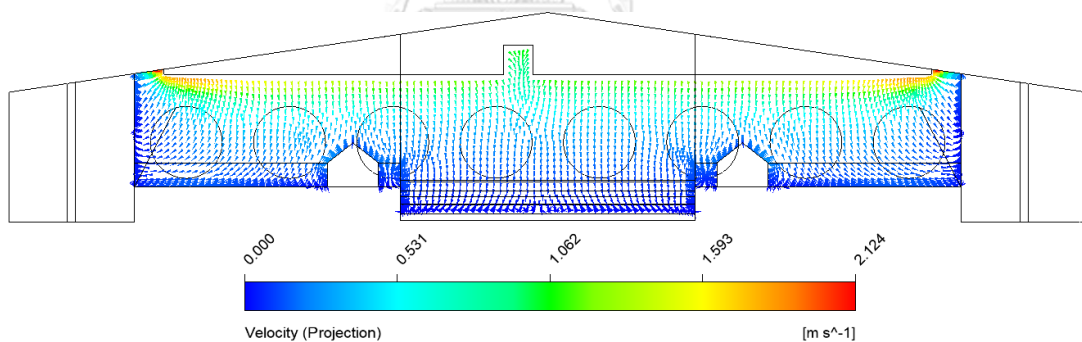


**Figure 4.7.10** Airflow direction from broad deflector at a vertical plane  $z = 81$  meters with longer deflectors when evaporative cooling pad and 12 exhausted fans operated.

(Note: external temperature and relative humidity are 41 degree Celsius and 40 percent, respectively.)

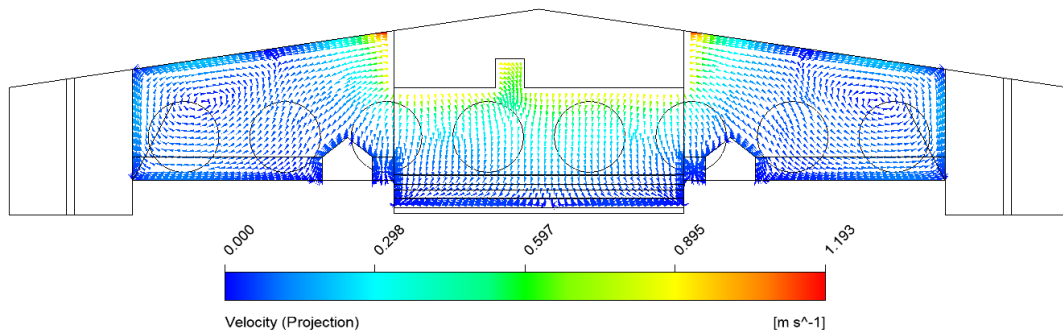


**Figure 4.7.11** Airflow direction from long deflector at a vertical plane  $z = 81$  meters with longer deflectors when evaporative cooling pad and 12 exhausted fans operated. (Note: external temperature and relative humidity are 41 degree Celsius and 40 percent, respectively.)

In conclusion, the broad deflector can increase the air velocity and enhance the uniformity of the air velocity profile at the chicken level. However, the air velocity beneath the first two deflector is very high, causing a non-uniform air velocity near the entrance. The first and second deflectors were modified by decreasing the length of the deflector in order to decrease the air velocity in this area. The length between the lower edge of the deflector and the floor is increased from 2.5 meters to 2.9 meters for the first deflector and 2.7 meters for the second deflector as shown in **Figure 4.7.12** and **4.7.13**. **Figure 4.7.14** illustrates the simulated air velocity at chicken level after the first and second deflector modification. The result shows that the modification can mitigate the high air velocity near the entrance. It is because the modification of the first two deflector increase the cross sectional area of airflow. Moreover, the area of the deflector is decreased. It caused the decrease in air dispersion to the middle and both sides of the chicken house. Therefore, the air velocity at the first two deflector is decreased and similar to other areas.

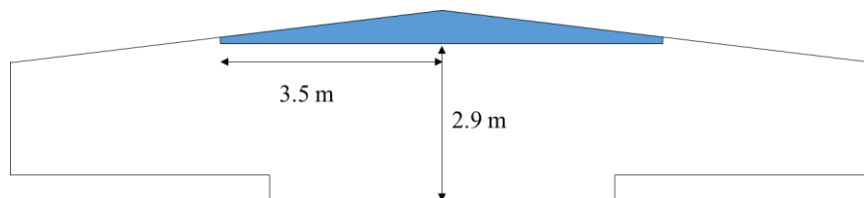


**Figure 4.7.12** First deflector after second modification

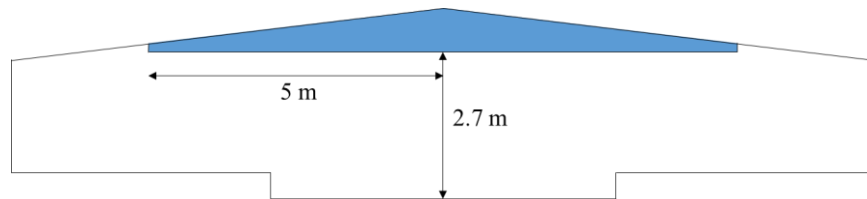


**Figure 4.7.13** Second deflector after second modification

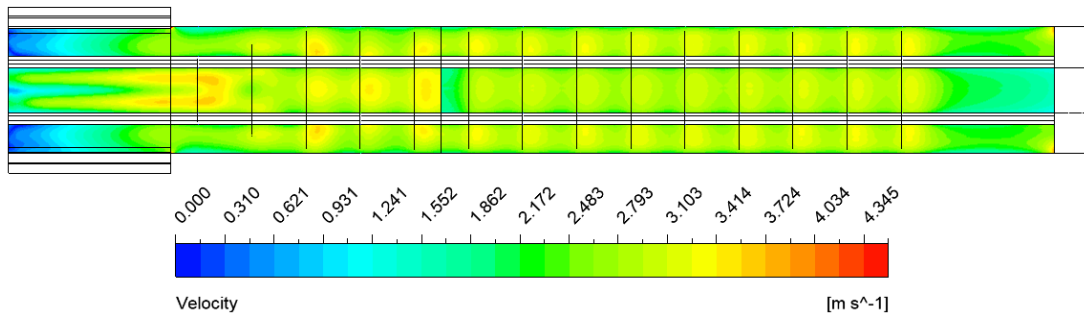


**Figure 4.7.14** Air velocity distribution at chicken level after the first and second deflector modification when evaporative cooling pad and 12 exhausted fans operated.

(Note: external temperature and relative humidity are 41 degree Celsius and 40 percent, respectively.)

**Figure 4.7.15** shows the effective temperature at the chicken level in the chicken house with broad deflector and the first two deflector modification. The effective temperature is greatly decreased when compared to the original house with original deflector. It shows that the air velocity plays an important role in improving climate inside the chicken house. Nevertheless, the effective temperature at the end of the house is higher than the optimal range, as a result of the increase in the air temperature from convective heat transfer.

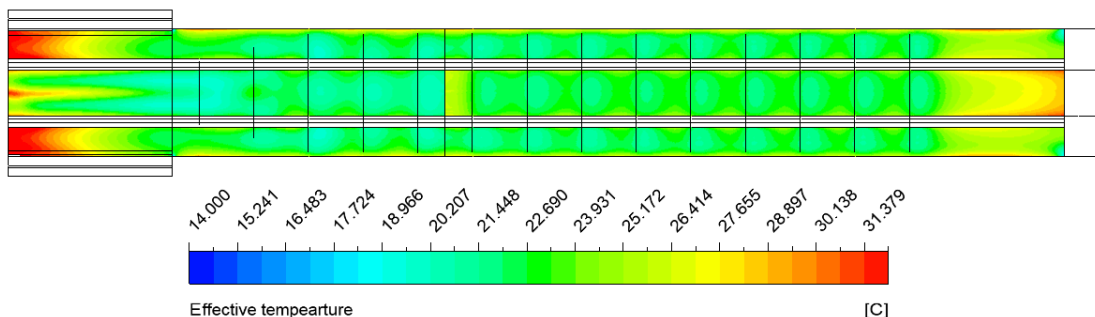


**Figure 4.7.15** Effective temperature distribution at chicken level in the chicken house with broad deflector and the first two deflector modification and without insulation when evaporative cooling pad and 12 exhausted fans operated. (Note: external temperature and relative humidity are 41 degree Celsius and 40 percent, respectively.)

### 4.7.3 Tunnel door modification

The tunnel door is installed at the inlet to mitigate the dead zone along both sides of the chicken house. Without a tunnel door the air would flow from the inlet straight to the end of the chicken house as shown in **Figure 4.7.16**. This flow pattern causes the air to mainly flow along the middle of the chicken house. Thus results in dead zone along both sides of the house as illustrated in **Figure 4.7.17**.

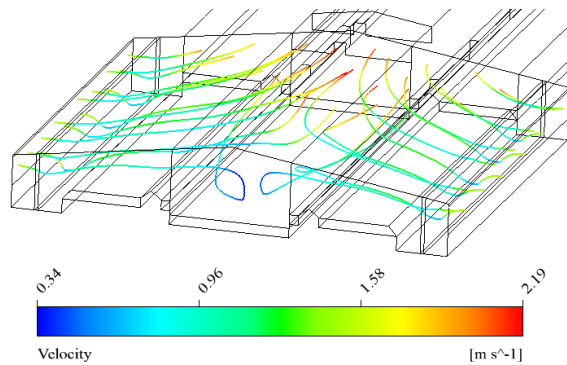


**Figure 4.7.16** Airflow pattern from the inlet through the chicken house without tunnel door when evaporative cooling pad are not operated and 8 exhaust fans are operated.

(Note: external temperature and relative humidity are 26.5 degree Celsius and 73 percent, respectively.)

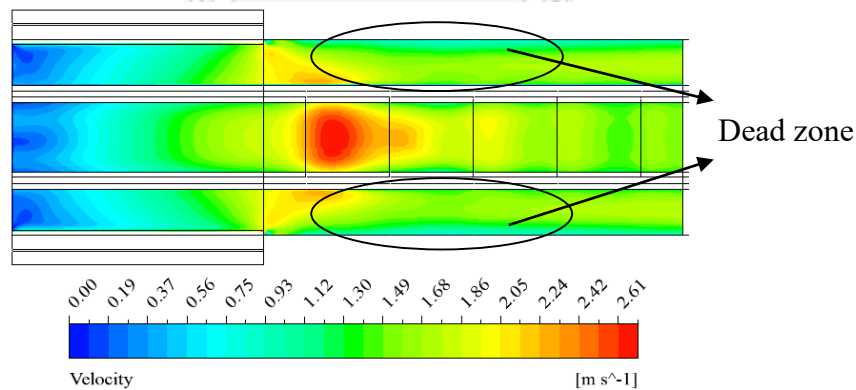


**Figure 4.7.17** Air velocity distribution at the chicken level in the chicken house without tunnel door when evaporative cooling pad are not operated and 8 exhaust fans are operated. (Note: external temperature and relative humidity are 26.5 degree Celsius and 73 percent, respectively.)

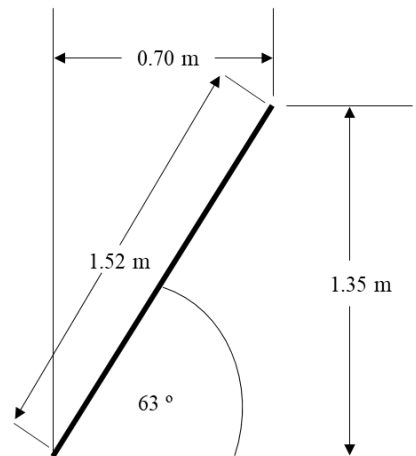


**Figure 4.7.18** Original tunnel door

The tunnel door can help mitigate the dead zone as previously discussed in **section 4.4.1**. However, it may cause the air at some locations in the first section of the chicken house to be at lower velocity compared to other areas. To solve this problem, the effect of tunnel door angle on the air velocity in the first section of the house was examined. The original inlet deflector can be shown in **Figure 4.7.18**. It was modified by varying the angle between the floor and tunnel door. The length was not changed. The modification was due to when the angle of the tunnel door is increased, the air velocity from the tunnel door is increased. The air velocity at the first section of the chicken house should be increased. The results of the modification can be illustrated as **Figure 4.7.19** and **Figure 4.7.20** for the path of airflow and contour of air velocity at the chicken level in the first section of the chicken house, respectively.

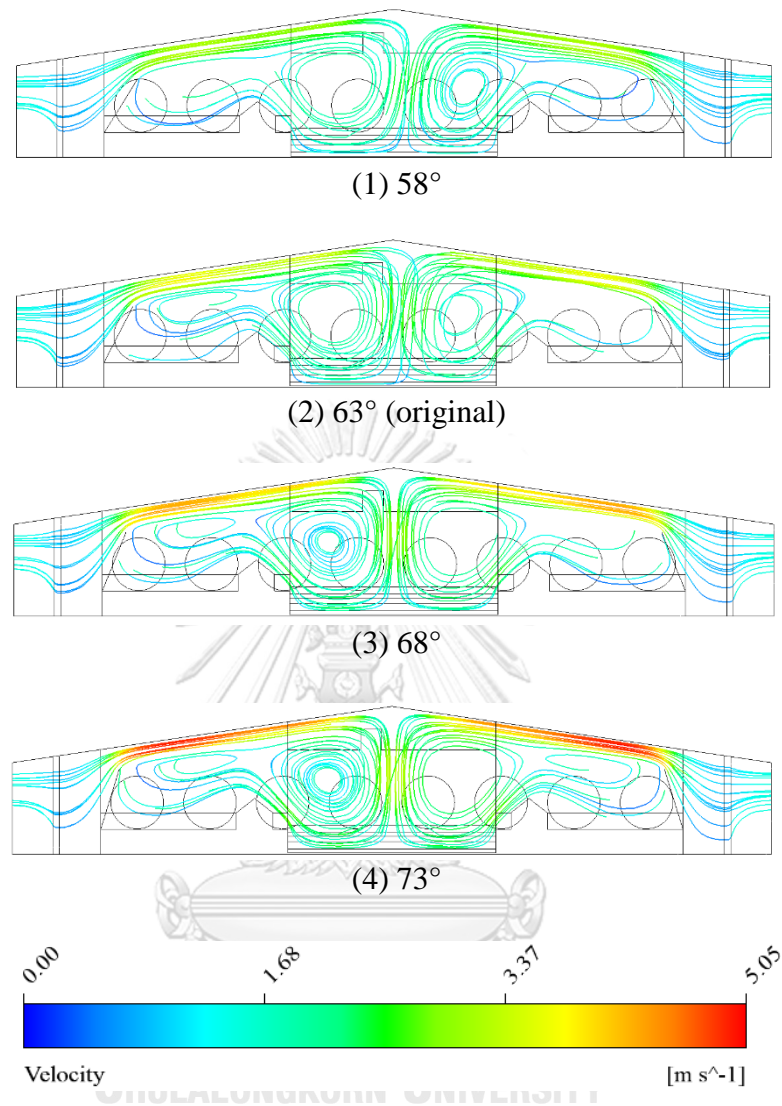


**Figure 4.7.19** Path of airflow after tunnel door modification when evaporative cooling pad are not operated and 8 exhaust fans are operated. (Note: external temperature and relative humidity are 26.5 degree Celsius and 73 percent, respectively.)

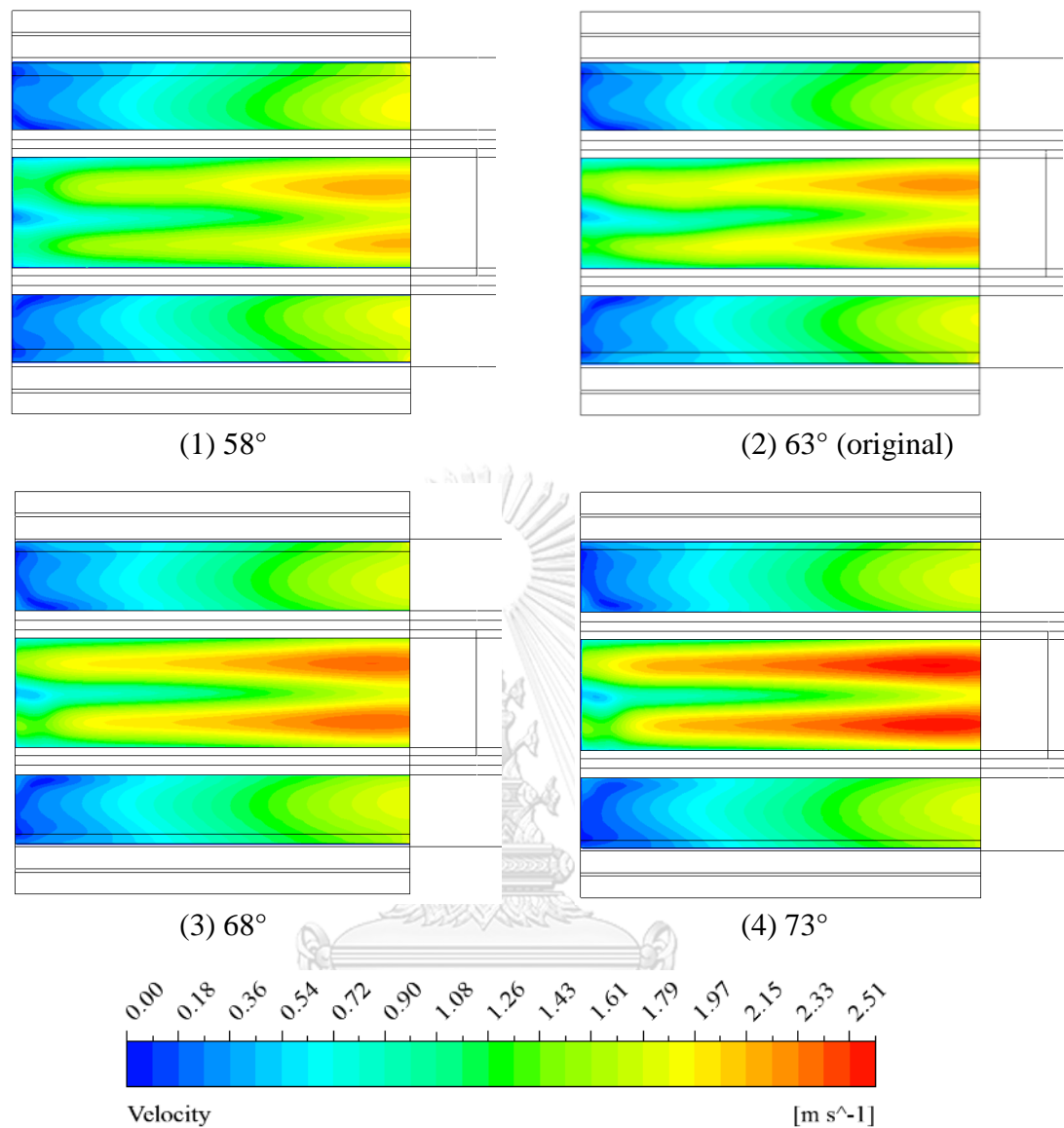


**Figure 4.7.20** Contour of air velocity at the chicken level after inlet deflector modification when evaporative cooling pad are not operated and 8 exhaust fans are operated. (Note: external temperature and relative humidity are 26.5 degree Celsius and 73 percent, respectively.)

From **Figure 4.7.19**, the path of airflow after the modification is still similar. However, the incoming air velocity magnitude from the tunnel door is different. With wider angle between the floor and tunnel door, a gap between the inlet deflector and the roof becomes narrower. Thus, the air flows through this gap at higher velocity. It results in higher air velocity in the middle of the first section of the chicken house as shown in **Figure 4.7.20**. This will worsen the non-uniform velocity profile near the

entrance as discussed in **section 4.7.2**. Further, the air velocity at the side of the house is still relatively similar. It can be implied by similar color gradients at the side of the house as shown **Figure 4.7.20**.

From **section 4.7.1 - 4.7.3**, the study confirms that the installation of thermal insulator can prevent the heat transfer from the roof into the chicken house significantly. In addition, the deflector modification can increase the air velocity and enhance uniform air velocity distribution at the chicken level. However, the inlet deflector modification cannot increase air velocity along the side of the first section of the chicken house. The effective temperature at the chicken level after the improvement which include an installation of 25-mm thick thermal insulation, a modification of deflector by width extension and the first two deflector shortening can be shown in **Figure 4.7.21**. In addition, the comparisons of effective temperature in the original and modified chicken houses are presented in **Figure 4.7.22**. The results show that the overall aforementioned improvement can reduce the effective temperature to within the optimal range of 20 – 24 degree Celsius along both sides and along the middle of the chicken house even when the outdoor climate is extreme (e.g., at a temperature of 41 degree Celsius and a relative humidity of 40 percent). However, there is an exception at the front end of the chicken house (effective temperature greater than 24 degree Celsius) because of the low air velocity in this area. This cannot be solved by modifying the angle of tunnel door.

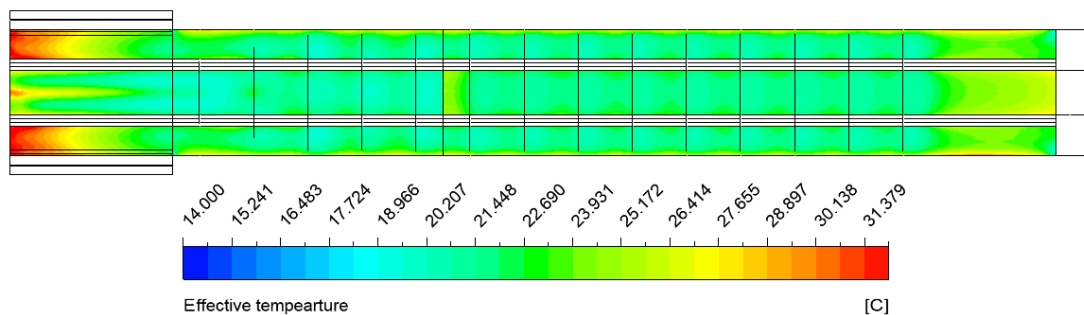


**Figure 4.7.21** Effective temperature distribution at chicken level after the thermal insulation, the deflector modification and the first two deflector modification when evaporative cooling pad and 12 exhausted fans operated. (Note: external temperature and relative humidity are 41 degree Celsius and 40 percent, respectively.)



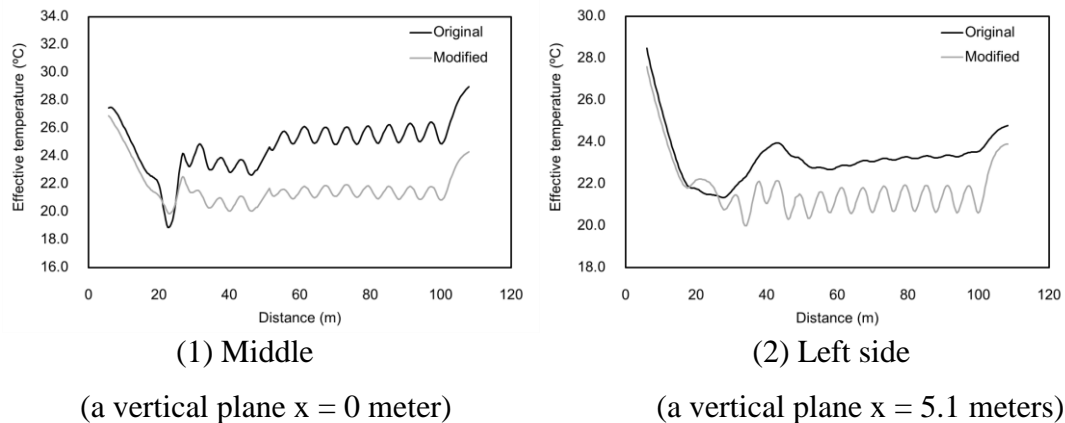
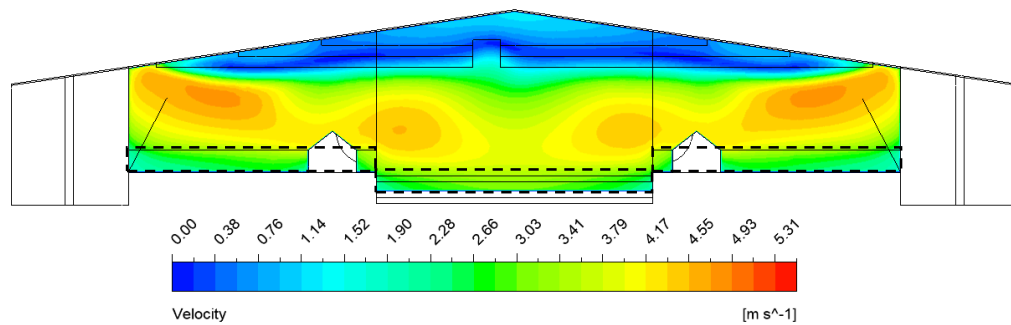
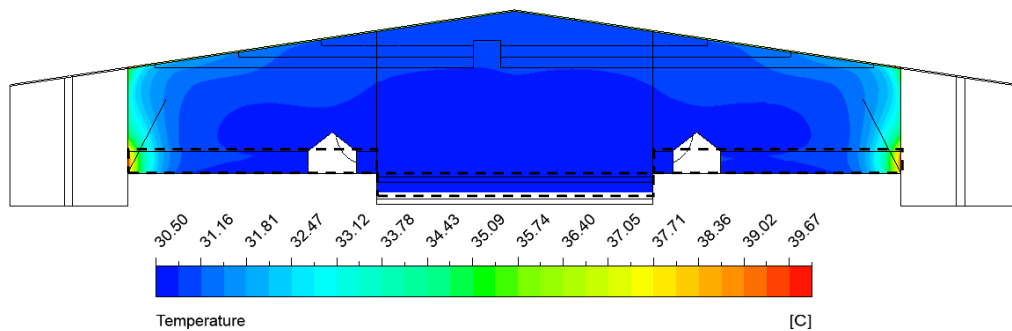


**Figure 4.7.22** Comparison of effective temperature at chicken level in original and modified chicken house when evaporative cooling pad and 12 exhausted fans operated. The modification includes the thermal insulation, the deflector modification and the first two deflector modification. (Note: external temperature and relative humidity are 41 degree Celsius and 40 percent, respectively.)

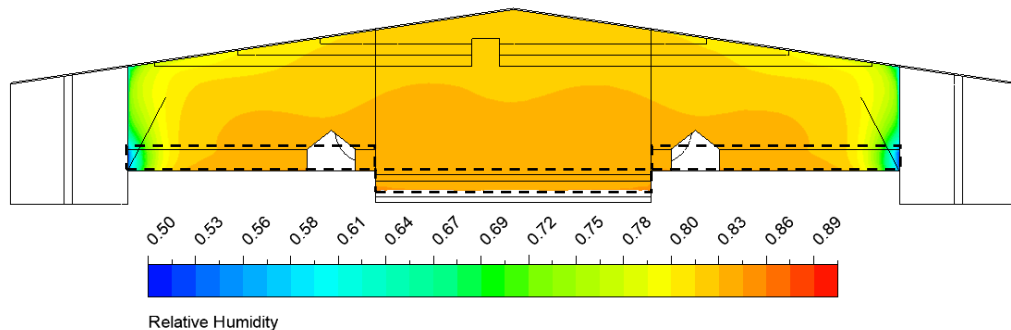
The contours of air velocity, temperature and relative humidity on vertical planes at  $z = 40$  meters (the front section of the chicken house) and at  $z = 80$  meters (the rear section of the house) are presented in **Figure 4.7.23** and **Figure 4.7.24**, respectively. The results show that the air velocity, temperature and relative humidity in the chicken occupied zone are distributed uniformly in the middle and on both sides of the chicken house. The maximum air velocity is at the sides of the chicken house on vertical planes at  $z = 40$  meters and  $z = 80$  meters. It is because the air is highly deflected at the sides of the chicken house as shown in **Figure 4.7.10**. However, the air velocity at the chicken level is similar on both sides and at the middle of the chicken house. Therefore, it does not affect the uniformity of the chicken. The air temperature on a vertical plane at  $z = 80$  meters is slightly higher than the air temperature on a vertical plane at  $z = 40$  meters. The airflow induces the heat convection which carries the emitted heat from the chicken to the outlet. Moreover, the heat transfer from the wall and roof also increases the air temperature. The relative humidity on a vertical plane at  $z = 80$  meters is lower than the relative humidity on a vertical plane at  $z = 40$  meters due to the increase in air temperature.



(1) Velocity



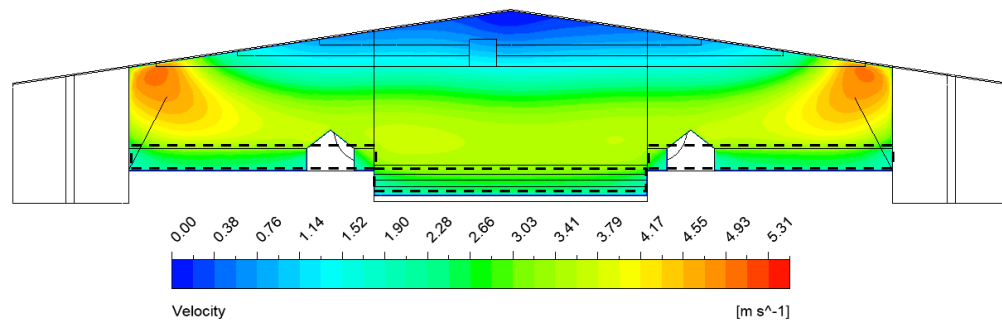
(2) Temperature



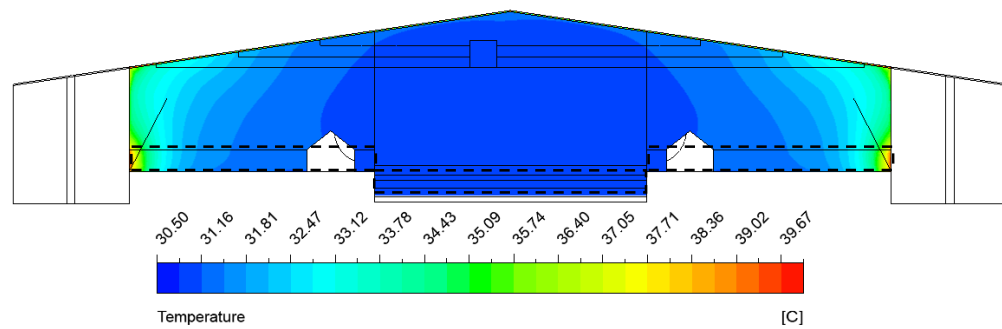
(3) Relative humidity

Dash line is chicken occupied zone.

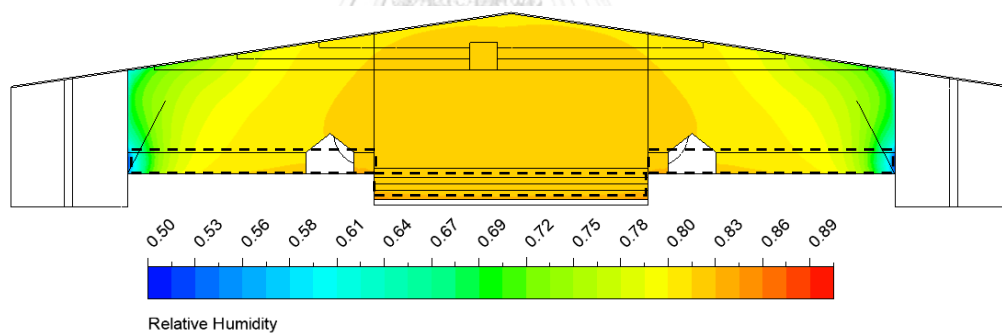
**Figure 4.7.24** Contours of air velocity, temperature and relative humidity on a vertical plane at  $z = 40$  meters in the chicken house with the thermal insulation, the broad deflector and the first two deflector modification when evaporative cooling pad and 12 exhausted fans operated. (Note: external temperature and relative humidity are 41 degree Celsius and 40 percent, respectively.)



(1) Air velocity



(2) Temperature



(3) Relative humidity

Dash line is chicken occupied zone.

**Figure 4.7.25** Contours of air velocity, temperature and relative humidity on a vertical plane at  $z = 80$  meters in the chicken house with the thermal insulation, the broad deflector and the first two deflector modification when evaporative cooling pad and 12 exhausted fans operated. (Note: external temperature and relative humidity are 41 degree Celsius and 40 percent, respectively.)

#### 4.7.4 Two-stage cooling system

In the preliminary study, the effect of the pipe length on the air temperature decrease was investigated by using CFD simulation. The pipe length was varied at 20, 25 and 30 meters. **Figure 4.7.26** shows the air temperature change along the 20-meter pipe. The outlet air temperature, relative humidity and the pressure drop are shown in **Table 4.7.1**.

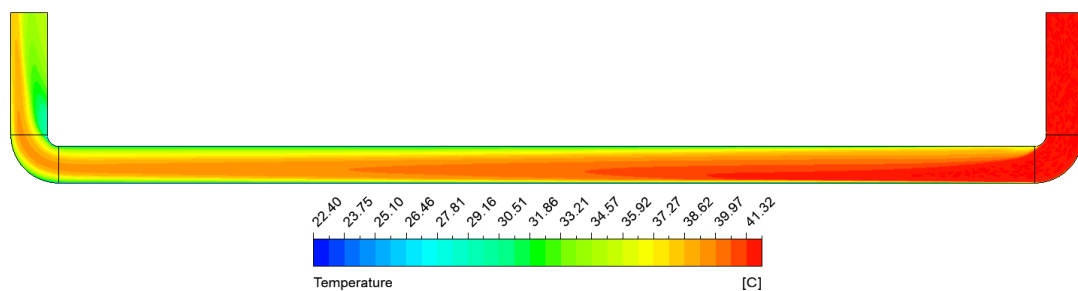


**Figure 4.7.26** A air temperature change along a 20-meter duct

**Table 4.7.1** Air temperature and relative humidity at the duct outlet and pressure drop

Pipe length (meters)	Air temperature at the pipe outlet (degree Celsius)	Relative humidity at the pipe outlet (percent)	Pressure drop (Pa)
20	34.75	57.6	20
25	35.49	55.3	23
30	36.31	52.9	25

(Inlet air temperature of 41 degree Celsius [55, 56])

From **Table 4.7.1**, the duct outlet temperature is decreased when the duct length is increased. This is because the longer pipe provides more heat transfer area. However, the longer pipe length causes higher pressure drop in the pipe. Thus, it requires more energy to operate the exhaust fan. Then, the air from the pipe flows to the evaporative cooling pad to further decrease the air temperature. **Table 4.7.2** shows the entry and exit air temperature for the evaporative cooling pad. The results are compared to the entry and exit temperature for the evaporative cooling pad in the original process (without the air-to-soil heat exchanging step). The results show that the exit air temperature from the evaporative cooling pad in the two-stage cooling system is lower than that from the pad in the original process by about 2 – 3 degree Celsius. This implies that the two-stage cooling system can help improve the air cooling efficiency.

**Table 4.7.2** Entry and exit air temperature for the evaporative cooling pad in the two stage cooling system with varied pipe lengths and in the original process without air-to-soil heat exchanging pipe

Duct length (meters)	Air temperature in front of the pad (degree Celsius)	Air temperature from the pad (degree Celsius)
20	34.75	28.86*
25	35.49	29.16*
30	36.31	29.50*
Original process	42.00	31.75*

\* At 85 percent evaporative cooling pad efficiency

However, other factors, such as pipe material (affecting thermal conductivity, strength and expenses) and the pipe number of pipe and size (affecting the pressure drop and the air flow rate fed to the chicken house) are also important and have not been tested. Therefore, further investigation for an optimal system design for the two-stage cooling system is still required.

## CHAPTER 5

# CONCLUSIONS AND RECOMMENDATION

### 5.1. Conclusions

This study was aimed to investigate the air velocity, temperature and relative humidity distribution inside the chicken house by using CFD modeling technique. The validated model was applied to simulate the indoor climate when the outdoor climate changed throughout the years. Moreover, the effects of extreme outdoor climate were also investigated to determine the factors which might help mitigate the thermal stress for the chicken. The conclusions of this study are written as follows:

- Realizable k- $\epsilon$ , energy conservation and species transport models were successfully applied to simulate momentum, energy and mass transport phenomena, respectively in the chicken house. The CFD model could predict the result well. Good agreements between simulation result and measured data were found (based on the values of NMSE).
- However, the air velocity at 1.4 meters height could not be predicted accurately. It was possibly due to the limitation of the air velocity sensor and the capability of the turbulence model to predict eddies from jet flow, which was caused by the influence of the deflectors.
- Porous media could effectively represent chicken occupied zone inside the chicken house. Discrete phase model was a suitable method for modeling the humidity emitted from the chicken.
- The validated model was successfully applied to develop an operational guideline to maintain a favorable climate for the chicken when the external climate changed throughout the years. From the simulation results, the original design chicken house could not provide suitable climate when the external temperature exceeded 39 degree Celsius at 30 – 40 percent relative humidity.

- The factors that cause the effective temperature to exceed the optimal range were the increase in temperature due to the heat transfer from the roof and insufficient air velocity blowing through the chicken occupied zone.
- An installation of thermal insulator could help prevent the heat transfer from the roof to the inside of the house effectively. The modification (i.e., expand the deflector width) to the deflectors could significantly increase the air velocity at the chicken level and enhance the uniformity of air velocity at the chicken level. However, changing the angle of the tunnel door could not improve the air velocity at the side of the first section (front end) of the chicken house.
- Two-stage cooling system could improve the air cooling efficiency. The air temperature was decreased by heat transfer from the air to the soil before it was further decreased by the evaporative cooling process. However, the two-stage cooling system proposed in this study still requires further investigated for optimal system design.

## 5.2 Recommendations

Although the Realizable  $k-\varepsilon$  model could well predict the air velocity at most locations in the chicken house, it still failed to predict the eddies under the deflectors accurately. A more complicated turbulence model, such as LES, would help improve the simulation accuracy in every area in the chick house, although at greater computational cost. The turbulence model with better prediction of flow under the deflectors might be applied to better craft the design of the deflectors.

The two-stage cooling system proposed here could significantly improve the air cooling efficiency. However, it still requires further investigation in various aspects; pipe material which affects thermal conductivity, strength and expense, optimal length and diameter of the pipe which affect pressure drop and air flow rate fed to evaporative cooling pad and thus affect ventilation in the chicken house. The additional study for optimal system design will be useful for improvement of the cooling system when the external climate is extreme.

## REFERENCES

1. World's Top exports. *Chicken exports by country*. 2017 [cited 2017 20 Dec]; Available from: <http://www.worldstopexports.com/chicken-exports-by-country/>.
2. *Thailand trading report (2018)*. 2018 [cited 2018 17 Nov]; Available from: [http://www.ops3.moc.go.th/export/recode\\_export\\_rank/](http://www.ops3.moc.go.th/export/recode_export_rank/).
3. Rojano, F., et al., *Modelling heat and mass transfer of a broiler house using computational fluid dynamics*. Biosystems Engineering, 2015. **136**: p. 25-38.
4. Seo, I.H., et al., *Improvement of the ventilation system of a naturally ventilated broiler house in the cold season using computational simulations*. Biosystems Engineering, 2009. **104**(1): p. 106-117.
5. Dawkins, M.S., C.A. Donnelly, and T.A. Jones, *Chicken welfare is influenced more by housing conditions than by stocking density*. Nature, 2004. **427**(6972): p. 342-4.
6. Xiong, Y., et al., *Effects of relative humidity on animal health and welfare*. Journal of Integrative Agriculture, 2017. **16**(8): p. 1653-1658.
7. Mashaly, M.M., et al., *Effect of Heat Stress on Production Parameters and Immune Responses of Commercial Laying Hens 1*. Poultry Science, 2004. **83**(6): p. 889-894.
8. Nardone, A., et al., *Effects of climate changes on animal production and sustainability of livestock systems*. Livestock Science, 2010. **130**(1-3): p. 57-69.
9. Heymsfield, C., *CFD Model for Ventilation in Broiler Holding Sheds*, in *Biological and Agricultural Engineering Undergraduate Honors Theses*. 2016.
10. Rojano, F., et al., *Test of two different schemes through CFD to include heat and mass transfer induced by animals inside a broiler house*. 2014.



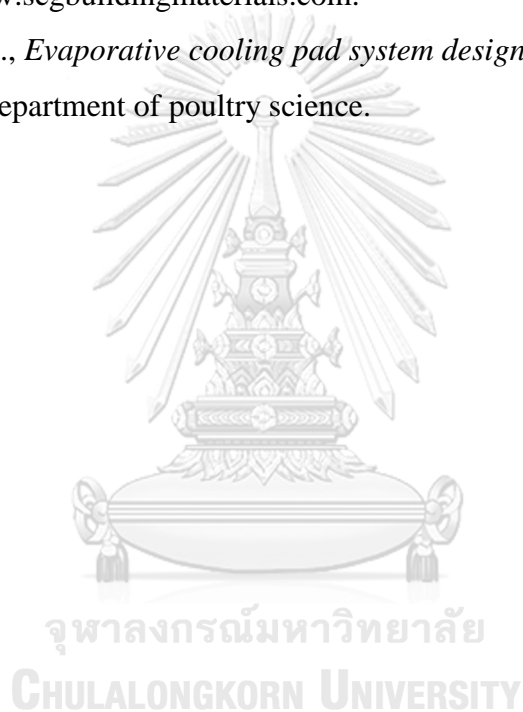
11. Rojano, F., et al., *Computational modelling of thermal and humidity gradients for a naturally ventilated poultry house*. Biosystems Engineering, 2016. **151**: p. 273-285.
12. Mostafa, E., et al., *Computational fluid dynamics simulation of air temperature distribution inside broiler building fitted with duct ventilation system*. Biosystems Engineering, 2012. **112**(4): p. 293-303.
13. Norton, T., et al., *Improving the representation of thermal boundary conditions of livestock during CFD modelling of the indoor environment*. Computers and Electronics in Agriculture, 2010. **73**(1): p. 17-36.
14. Saraz, O., et al., *Use of computational fluid dynamics to simulate temperature distribution in broiler houses with negative and positive tunnel type ventilation systems*. Revista UDCA Actualidad & Divulgación Científica, 2013. **16**(1): p. 159-166.
15. Bustamante, E., et al., *Measurement and Numerical Simulation of Air Velocity in a Tunnel-Ventilated Broiler House*. Sustainability, 2015. **7**(12): p. 2066-2085.
16. Tinoco, I.D.F.F., et al. *3D-CFD modeling of a typical uninsulated and internal misting tunnel ventilated brazilian poultry house*. in *2010 Pittsburgh, Pennsylvania, June 20-June 23, 2010*. 2010. American Society of Agricultural and Biological Engineers.
17. Zajicek, M. and K. Pavel, *Longitudinal ventilation of broiler house—simulation of variants*. Engineering for Rural Development, Jelgava, 2013: p. 23-24.05.
18. Osorio Hernandez, R., et al., *CFD modeling of the thermal environment in a negative pressure tunnel ventilated broiler barn during the first week of life*. 2015.
19. Blanes-Vidal, V., et al., *Application of computational fluid dynamics to the prediction of airflow in a mechanically ventilated commercial poultry building*. Biosystems Engineering, 2008. **100**(1): p. 105-116.
20. Fidaros, D., et al., *Numerical study of mechanically ventilated broiler house equipped with evaporative pads*. Computers and Electronics in Agriculture, 2018. **149**: p. 101-109.

21. J. L. Purswell, B.D.L., J. D. Davis, *Effect of Air Deflectors on Fan Performance in Tunnel-Ventilated Broiler Houses with a Dropped Ceiling*. Applied Engineering in Agriculture, 2014: p. 471-475.
22. Zou, H., et al. *CFD Simulation of the Airflow in Poultry Housing with Wind Shield*. in *Proceedings of the 8th International Symposium on Heating, Ventilation and Air Conditioning*. 2014. Springer.
23. May, J.D., B.D. Lott, and J.D. Simmons, *The effect of air velocity on broiler performance and feed and water consumption I*. Poultry Science, 2000. **79**(10): p. 1396-1400.
24. Pereira, D.F. and I.A. Nääs, *Estimating the thermoneutral zone for broiler breeders using behavioral analysis*. Computers and Electronics in Agriculture, 2008. **62**(1): p. 2-7.
25. Furlan, R.L., et al., *Air Velocity and Exposure Time to Ventilation Affect Body Surface and Rectal Temperature of Broiler Chickens*. The Journal of Applied Poultry Research, 2000. **9**(1): p. 1-5.
26. Yahav, S., et al., *Air Velocity Alters Broiler Performance Under Harsh Environmental Conditions*. Vol. 80. 2001. 724-6.
27. Timmons, M.B. and P.E. Hillman, *Tunnel ventilation revisited in prevention of heat stress*. Poultry Digest, 1993: p. 5216-19.
28. Tao, X. and H. Xin. *Temperature-Humidity-Velocity Index for Market-size Broilers*. in *Agricultural and Biosystems Engineering Conference Proceedings and Presentations*. 2003.
29. D Kabuga, J., *The influence of thermal conditions on rectal temperature, respiration rate and pulse rate of lactating Holstein-Friesian cows in the humid tropics*. Vol. 36. 1992. 146-50.
30. Ingram, D.L., *The effect of humidity on temperature regulation and cutaneous water loss in the young pig*. Research in Veterinary Science, 1965. **6**: p. 9-17.
31. Zulovich, J.M. and J.A. DeShazer, *Estimating egg production declines at high environmental temperatures and humidities*. 1990. p. 15 pp.
32. Stull, R., *Wet-Bulb Temperature from Relative Humidity and Air Temperature*. Journal of Applied Meteorology and Climatology, 2011. **50**(11): p. 2267-2269.

33. *Effective temperature*. BFI7. Retrieved from farm database.
34. Kovačević, I. and M. Sourbron, *The numerical model for direct evaporative cooler*. Applied Thermal Engineering, 2017. **113**: p. 8-19.
35. Wu, W., et al., *Evaluation of methods for determining air exchange rate in a naturally ventilated dairy cattle building with large openings using computational fluid dynamics (CFD)*. Atmospheric Environment, 2012. **63**: p. 179-188.
36. Li, H., L. Rong, and G. Zhang, *Numerical study on the convective heat transfer of fattening pig in groups in a mechanical ventilated pig house*. Computers and Electronics in Agriculture, 2017.
37. Li, H., L. Rong, and G. Zhang, *Reliability of turbulence models and mesh types for CFD simulations of a mechanically ventilated pig house containing animals*. Biosystems Engineering, 2017. **161**: p. 37-52.
38. Rong, L., B. Bjerg, and G. Zhang, *Assessment of modeling slatted floor as porous medium for prediction of ammonia emissions – Scaled pig barns*. Computers and Electronics in Agriculture, 2015. **117**: p. 234-244.
39. Kwon, K.-s., et al., *Computational fluid dynamics analysis of the thermal distribution of animal occupied zones using the jet-drop-distance concept in a mechanically ventilated broiler house*. Biosystems Engineering, 2015. **136**: p. 51-68.
40. Bustamante, E., et al., *Measurement and numerical simulation of single-sided mechanical ventilation in broiler houses*. Biosystems Engineering, 2017. **160**: p. 55-68.
41. Versteeg, H.K. and W. Malalasekera, *An introduction to computational fluid dynamics: the finite volume method*. 2007: Pearson Education.
42. Norton, T., et al., *Applications of computational fluid dynamics (CFD) in the modelling and design of ventilation systems in the agricultural industry: a review*. Bioresour Technol, 2007. **98**(12): p. 2386-414.
43. Zong, C. and G. Zhang, *Numerical modelling of airflow and gas dispersion in the pit headspace via slatted floor: Comparison of two modelling approaches*. Computers and Electronics in Agriculture, 2014. **109**: p. 200-211.

44. Rong, L., et al., *Summary of best guidelines and validation of CFD modeling in livestock buildings to ensure prediction quality*. Computers and Electronics in Agriculture, 2016. **121**: p. 180-190.
45. Cheng, Q., et al., *CFD study of the influence of laying hen geometry, distribution and weight on airflow resistance*. Computers and Electronics in Agriculture, 2018. **144**: p. 181-189.
46. Ntinias, G.K., et al., *Evaluation of CFD turbulence models for simulating external airflow around varied building roof with wind tunnel experiment*. Building Simulation, 2017. **11**(1): p. 115-123.
47. Mendes, L., et al., *Air motion patterns in a naturally ventilated dairy barn by means of a cfd model combined with the carbon dioxide mass balance method*. 2014.
48. Walsberg, G.E., *The Relationship of the External Surface Area of Birds to Skin Surface Area and Body Mass*. The Journal of Experimental Biology, 1978. **76**(1): p. 185.
49. Pedersen, S. and K. Sällvik, *Heat and moisture production at animal and house levels*. 2002.
50. Meda, B., *A dynamic approach of nutrients and energy flows in poultry rearing systems: Conception and application of the model MOLDAVI*. 2011, Agrocampus Ouest.
51. *Euroemme fan specification*. BFI7. Retrieved from farm database.
52. Franco, A., et al., *Aerodynamic analysis and CFD simulation of several cellulose evaporative cooling pads used in Mediterranean greenhouses*. Computers and Electronics in Agriculture, 2011. **76**(2): p. 218-230.
53. Florides, G.A. and S.A. Kalogirou, *Annual ground temperature measurements at various depths*. 2005.
54. Alchalabi, D., *Cooling Poultry Houses Basic Principles of Humidity and Temperature*. 2015.
55. van Hooff, T., B. Blocken, and Y. Tominaga, *On the accuracy of CFD simulations of cross-ventilation flows for a generic isolated building: Comparison of RANS, LES and experiments*. Building and Environment, 2017. **114**: p. 148-165.

56. *Pak Chong Historical Weather*. [cited 2018 Jul]; Available from: <https://www.wunderground.com/weather/th/pak-chong>.
57. *Weather in Amphoe Pak Chong*. [cited 2018 Jul]; Available from: <https://www.timeanddate.com/weather/@1608056>.
58. *Thailand Annual Weather Summary, 2015*. 2016, Climatological Center, Meteorological Development Bureau.
59. Thakerd, S., *Personal communication*. 2018.
60. *Thermal insulation for roof [Brochure]*. Available from: <https://www.scgbuildingmaterials.com>.
61. Czarick, M., *Evaporative cooling pad system design 2014*. The university of Georgia, Department of poultry science.



## REFERENCES



จุฬาลงกรณ์มหาวิทยาลัย  
**CHULALONGKORN UNIVERSITY**

# Appendix A

## A.1 Effective temperature data from farm

EFFECTIVE TEMPERATURE FROM EACH TEMPERATURE AND % RELATIVE HUMIDITY RANGE

95

Ambient temp. & % Rel Hum		Number of Fan Run AND air velocity inside the House (ft./min.)										
Temperature (°C)	% Relative Humidity	0	1	2	3	4	5	6	7	8	9	10
35	<50	35.00	33.60	32.20	29.40	26.60	25.50	24.40	23.90	23.30	22.80	22.20
	50-70	36.65	35.30	33.90	31.20	28.60	27.60	26.60	25.70	24.70	24.00	23.30
	>70	38.30	36.90	35.50	33.00	30.50	29.70	28.80	27.50	26.10	25.30	24.40
34.3	<50	34.30	32.90	31.50	28.90	26.40	25.30	24.30	23.70	23.20	22.60	21.90
	50-70	36.00	34.60	33.20	30.70	28.20	27.30	26.30	25.60	24.60	23.80	23.00
	>70	37.60	36.20	34.80	32.40	30.10	29.20	28.40	27.20	26.00	25.00	24.10
33.6	<50	33.60	32.20	30.80	28.50	26.10	25.10	24.20	23.60	23.10	22.40	21.70
	50-70	35.30	33.90	32.50	30.20	27.90	27.00	26.10	25.30	24.40	23.60	22.80
	>70	36.90	35.50	34.10	31.90	29.70	28.80	28.00	26.90	25.80	24.80	23.90
32.9	<50	32.90	31.50	30.10	28.00	25.90	24.90	24.00	23.50	22.90	22.20	21.40
	50-70	34.55	33.20	31.80	29.60	27.50	26.70	25.80	25.10	24.30	23.40	22.50
	>70	36.20	34.80	33.40	31.30	29.20	28.40	27.60	26.60	25.70	24.60	23.60
32.2	<50	32.20	30.80	29.40	27.50	25.60	24.80	23.90	23.40	22.80	22.00	21.10
	50-70	33.85	32.60	31.10	29.10	27.20	26.40	25.60	24.90	24.20	23.20	22.20
	>70	35.50	34.10	32.70	30.80	28.80	28.00	27.20	26.40	25.50	24.40	23.30
31.5	<50	31.50	30.10	28.70	27.00	25.30	24.50	23.60	23.00	22.40	21.80	20.80
	50-70	33.00	31.70	30.40	28.60	26.90	26.00	25.20	24.50	23.80	22.90	22.10
	>70	34.50	33.30	32.00	30.20	28.40	27.60	26.80	26.00	25.20	24.30	23.30
30.8	<50	30.80	29.40	28.00	26.50	25.00	24.20	23.40	22.70	22.00	21.30	20.60
	50-70	32.20	30.90	29.70	28.10	26.50	25.70	24.90	24.20	23.50	22.70	21.90
	>70	33.60	32.50	31.40	29.70	28.00	27.20	26.40	25.70	25.00	24.10	23.30
29.4	<50	29.40	28.00	26.60	25.50	24.40	23.60	22.80	22.00	21.10	20.60	20.00
	50-70	30.60	29.40	28.30	27.10	26.00	25.00	24.20	23.60	22.80	22.20	21.70
	>70	31.60	30.80	30.00	28.60	27.20	26.40	25.50	25.00	24.40	23.90	23.30
28.7	<50	28.70	27.40	26.10	25.00	23.90	23.10	22.40	21.50	20.80	20.10	19.80
	50-70	29.70	28.60	27.50	26.40	25.10	24.40	23.70	22.80	22.00	21.50	21.00
	>70	30.80	29.90	29.00	27.80	26.90	26.70	25.00	24.20	23.40	22.90	22.30
28	<50	28.00	26.80	25.50	24.40	23.30	22.60	22.00	21.00	20.00	19.60	19.20
	50-70	29.00	27.90	26.80	25.70	24.60	23.90	23.20	22.20	21.20	20.70	20.30
	>70	30.00	29.00	28.10	26.90	25.80	25.10	24.40	23.40	22.50	21.90	21.40
27.3	<50	27.30	26.10	25.00	23.90	22.80	22.10	21.50	20.50	19.50	19.10	18.70
	50-70	28.20	27.10	26.00	25.00	23.90	23.30	22.70	21.60	20.50	20.00	19.60
	>70	29.10	28.10	27.20	26.10	25.10	24.50	23.90	22.70	21.50	20.90	20.40
26.6	<50	26.60	25.50	24.40	23.30	22.20	21.70	21.10	20.00	18.90	18.60	18.30
	50-70	27.50	26.40	25.30	24.30	23.30	22.80	22.20	21.00	19.70	19.30	18.90
	>70	28.30	27.20	26.10	25.30	24.40	23.90	23.30	21.90	20.50	20.00	19.40
25.9	<50	25.90	25.00	24.00	23.00	21.90	21.40	20.80	19.70	18.60	18.20	17.90
	50-70	26.80	25.80	24.80	23.90	23.00	22.50	21.90	20.70	19.50	19.00	18.60
	>70	27.60	26.60	25.70	24.90	24.10	23.60	23.00	21.70	20.40	19.80	19.30
25.3	<50	25.30	24.40	23.60	22.60	21.70	21.10	20.60	19.40	18.30	17.90	17.50
	50-70	26.10	25.30	24.40	23.60	22.80	22.20	21.70	20.60	19.30	18.80	18.30
	>70	26.90	26.10	25.30	24.60	23.90	23.30	22.80	21.50	20.30	19.70	19.10
24.6	<50	24.60	23.90	23.20	22.30	21.40	20.80	20.30	19.10	18.00	17.50	17.00
	50-70	25.40	24.70	24.00	23.20	22.50	21.90	21.40	20.20	19.10	18.50	18.00
	>70	26.20	25.50	24.80	24.20	23.60	23.00	22.50	21.30	20.10	19.50	19.00
23.9	<50	23.90	23.40	22.80	22.00	21.10	20.60	20.00	18.90	17.70	17.20	16.60
	50-70	24.70	24.20	23.60	22.90	22.20	21.70	21.10	20.00	18.90	18.30	17.70
	>70	25.50	25.00	24.40	23.90	23.30	22.80	22.20	21.10	20.00	19.40	18.80

Figure A.1 Effective temperature data

## Appendix B

### B.1 Evaporative cooling pad efficiency statistical analysis

Normally, the evaporative cooling pad efficiency depends on incoming air velocity, temperature and relative humidity [34]. However, in this study, the evaporative cooling pad efficiency was assumed to be 85 percent which represents the efficiency at every climate condition. In order to prove this assumption, Duncan's mean separation test was applied by comparing the air temperature from the pad at 85 percent efficiency with the air temperature calculated from numerical model [34] and evaporative cooling pad system design [61].

Duncan's mean separation test is the hypothesis test by computing the significant mean difference calculated from different method. The computation detail can be expressed by following.

1. The average of air temperature from the pad at various external climate which is calculated from different method can be shown as **Table B.1**. The air velocity is defined as 1 m/s.

**Table B.1** Air temperature from the pad at various external climate

Incoming air temperature (degree Celsius)	Numerical model			Evaporative cooling pad system design			85 percent efficiency		
	Relative humidity (percent)			Relative humidity (percent)			Relative humidity (percent)		
	30	50	70	30	50	70	30	50	70
48	31.1	37.2	42.1	35.1	39.3	43.0	34.4	39.3	43.2
44	28.2	33.8	38.4	31.9	35.8	39.3	31.2	35.8	39.4
40	25.3	30.5	34.7	28.7	32.3	35.6	28.0	32.3	35.7
36	22.5	27.1	31.1	25.5	28.9	31.9	24.9	28.7	31.9
32	19.6	23.8	27.4	22.3	25.4	28.2	21.7	25.2	28.1
28	16.8	20.5	23.8	19.1	21.9	24.5	18.5	21.7	24.4
24	13.9	17.2	20.1	15.8	18.5	20.8	15.4	18.2	20.6
20	11.1	13.9	16.5	12.6	15.0	17.1	12.2	14.6	16.8
Average	25.3			27.0			26.76		



2. Sort the average air temperature in descending

Evaporative cooling pad system design (A)	85 percent efficiency	Numerical model
27.0	26.76	25.3

3. Calculate the critical value ( $q_{\alpha,k,v}$ ) from Significant studentized range table. The significant level ( $\alpha$ ) was defined as 0.05.  $k$  is the interval between dataset (2,3, ...,  $t$ ) when  $t$  is the total dataset.  $v$  is degree of freedom.

$k$	2	3
$(q_{0.05,k,69})$	2.8214	3.3875

4. Calculate critical range ( $CR_k$ ) when  $(CR_k) = q_{\alpha,k,v} \sqrt{\frac{MSE}{rep}}$ .  $rep$  is number of the data in one dataset minus one.

$k$	2	3
$CR_k$	4.9707	5.9681

5. Compare the difference between the average and ( $CR_k$ ).

	Mean difference	$CR_k$
Mean A – Mean C	1.70	< 5.9681
Mean A – Mean B	0.24	< 4.9707
Mean B – Mean C	1.46	< 4.9707

From the comparison, the mean difference is less than  $CR_k$ . It can be conclude that there is no significant difference between the average air temperatures from the pad by calculating from three different method. Therefore, the assumption which is defined the evaporative cooling pad efficiency equal to 85 percent is acceptable.

## Appendix C

### C.1 Example of operating guideline consideration

The external temperature and relative humidity is 24 degree Celsius and 60 percent, respectively. The number of operating fans is 6 fans and the evaporative cooling pad system is not operated. The air velocity, temperature, relative humidity and effective temperature at the chicken level are shown as **Figure C.1 – C.4**.

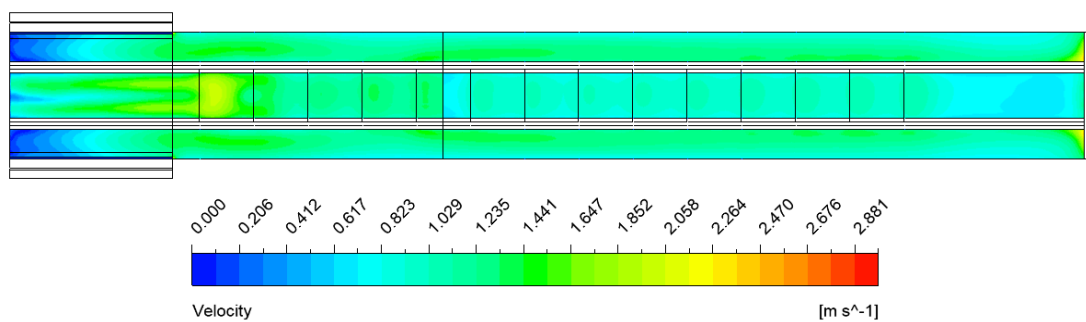


**Figure C.1** Air velocity distribution at chicken level

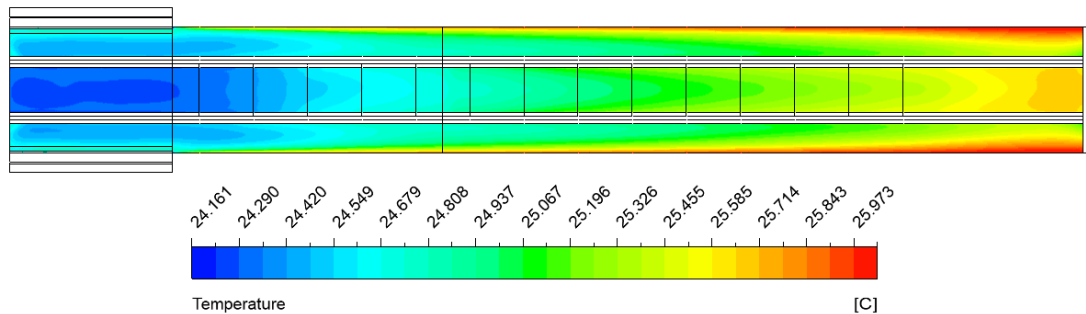


**Figure C.2** Temperature distribution at chicken level

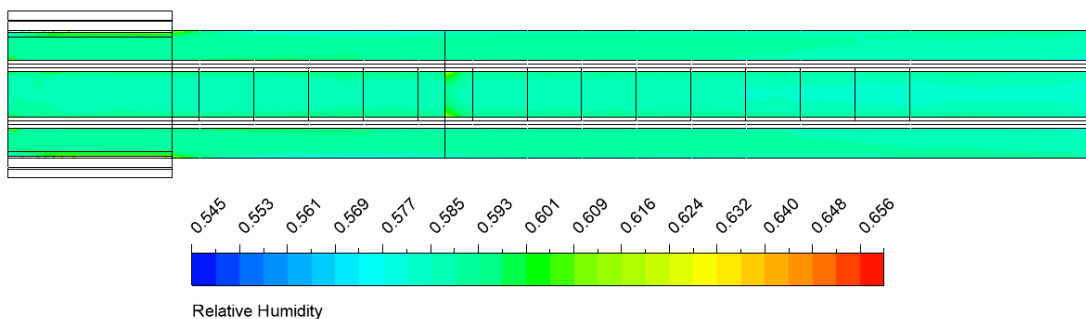


**Figure C.3** Relative humidity distribution at chicken level

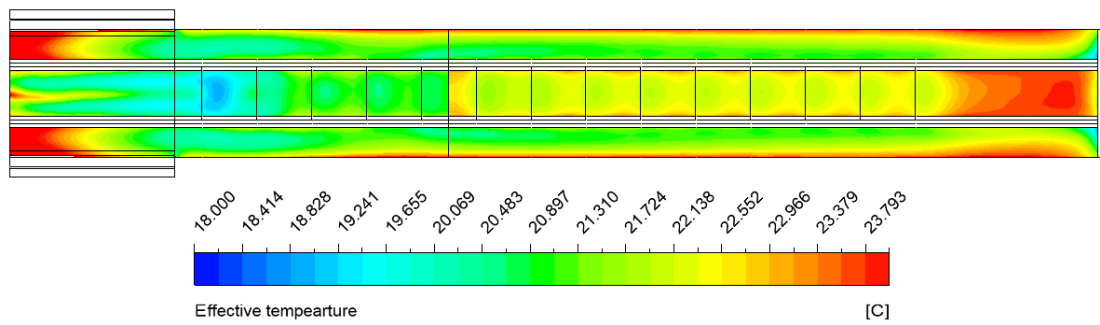


**Figure C.4** Effective temperature distribution at chicken level

From Figure A.4, the effective temperature at most of areas inside the house is within the optimal range ( $21\pm 3$ ) when the operating fans is 6 fans and the evaporative cooling pad system is not operated.





จุฬาลงกรณ์มหาวิทยาลัย  
**CHULALONGKORN UNIVERSITY**

## VITA

**NAME** Nuttahpon Kanjanaudomsuk

**DATE OF BIRTH** 29 March 1994

**PLACE OF BIRTH** Bangkok, Thailand

**INSTITUTIONS  
ATTENDED** Chemical engineering, Faculty of Engineering,  
Chulalongkorn University

**HOME ADDRESS** 56/20 Jakkraphet rd. Wangburapapirom Pranakorn  
Bangkok 10200



จุฬาลงกรณ์มหาวิทยาลัย  
CHULALONGKORN UNIVERSITY